Master's thesis

NTNU
Norwegian University of Science and Technology
Faculty of Information Technology and Electrical Engineering
Department of Electric Power Engineering

Helene Grimstad Osberg

New Environmentally-friendly Insulation Gases

Breakdown Mechanisms along Insulating Cylinders when implementing Barriers and Triple Junction Gaskets

Master's thesis in Energy and Environmental Engineering
Supervisor: Frank Mauseth
Co-supervisor: Hans Kristian Hygen Meyer
June 2023

NTNU
Norwegian University of
Science and Technology

Helene Grimstad Osberg

New Environmentally-friendly Insulation Gases

Breakdown Mechanisms along Insulating Cylinders when implementing Barriers and Triple Junction Gaskets

Master's thesis in Energy and Environmental Engineering
Supervisor: Frank Mauseth
Co-supervisor: Hans Kristian Hygen Meyer
June 2023

Norwegian University of Science and Technology
Faculty of Information Technology and Electrical Engineering
Department of Electric Power Engineering

NTNU
Norwegian University of Science and Technology

Preface

This thesis has been completed at the Department of Electric Energy at the Norwegian University of Science and Technology.

I would like to thank my supervisor Frank Mauseth, at NTNU and co-supervisor Hans Kristian Meyer, at SINTEF Energy Research for their help with the project and their encouragement and expertise when the results were not as expected.

I would also like to thank the service lab for without them my project would not be possible. I would especially like to thank Morten Flå and Dominik Häger for their immense help with the test object. I would like to thank Bård Almås for his help with the AC test setup.

Lastly, I would like to thank my fellow students in F312 for their motivation and support.

Helene G. Osberg

Helene G. Osberg

Trondheim, June 2023

Abstract

SF_6 is a potent greenhouse gas used in medium voltage gas insulated switchgear. SF_6 will likely be more strongly regulated in the future. New environmentally friendly gases, like pressurised air, should be investigated to replace SF_6. Air has a lower withstand voltage than SF_6, so when implementing air as an insulating gas, an understanding of the breakdown mechanism is needed. The breakdown strength of some of the weakest parts of the insulation systems, the gas-solid interface, should be improved to keep the dimensions of the switchgear.

The objective of this thesis is to investigate if adding barriers or gaskets to an insulating cylinder can increase the breakdown strength of an air gap with a solid-gas interface. Barriers were placed around a profiled insulating cylinder. The gaskets were either rubber or silicone and placed at the triple junction (gas-metal-insulator interface) of a smooth cylinder. Up-and-down tests were completed on the test object to find the 50% breakdown voltage. COMSOL Multiphysics simulations were computed to supplement the breakdown voltage experiments for gaskets. The inception voltage was calculated using a Python script implementing the streamer inception criteria. The AC average breakdown voltage was found using a continuous rising method for the silicone gaskets.

The breakdown voltage did not increase when adding a 3D-printed, PLA barrier around the insulating cylinder. The breakdown channels were located between the cylinder and the barrier, hindering an increase in breakdown voltage.

The breakdown voltage did slightly increase with pre-fabricated NBR rubber gaskets. The rubber gaskets at a pure triple junction are very sensitive to minute variations in the placement and shape of the gasket. The gain achieved using rubber gaskets is small. COMSOL simulations confirmed an increase in inception voltage with certain gasket conditions.

The breakdown voltage increased 20% with silicone gaskets that were cast directly on the test object. Slight variations in the gasket geometry did not affect the voltage. The inception voltages coincide with where the streamers propagate. The results indicate the elimination of the field enhancements at the triple junctions. An increase in breakdown voltage up to 24% during AC operation with the silicone gaskets was observed.

Sammendrag

SF_6 er en kraftig drivhusgass, som benyttes i mellomspennings gasisolerte koblingsanlegg. Det er sannsynlig at SF_6 kommer til å bli strengere regulert i fremtiden. Nye miljøvennlige isolasjonsajonsgasser, som trykksatt luft burde undersøkes som alternativer til SF_6. Luft har lavere holfasthet, så for å gjennomføre en overgang til luft som isolasjonsgass må overgslagsmekanismene undersøkes. Overslagsspenningen til noen av de svakeste delene av et isolasjonssystem, overflaten mellom gas og fast material må undersøkes for å beholde dimensjonene til koblingsanlegget.

Målet med avhandlingen er å undersøke om det å benytte barrierer eller pakninger rundt en isolasjonsylinder kan øke overslagsspenningen til et luftgap med et isolasjonsmateriale i fast form. Barrierer ble plassert rundt en profilert isolajsonssylinder. Pakningene av enten gummi eller silikon, ble plassert ved trippelpunktet til en glatt sylinder. Opp-og-ned tester ble gjennomført for å finne 50% overslagsspenning. COMSOL Multiphysics simuleringer av de elektriske feltene rundt pakningene ble gjennomført som et supplement til overslagsspennigene. Tennspenningen ble beregnet ved hjelp av et Python-skript ved hjelp av streamerinitiereingskriteriet. Gjennomsnittlig AC-overslagspenning ble funnet ved bruk av kontinuerlig økning spenning fram til overslag for silikonpakningene.

Overslagsspenningen økte ikke ved å legge til en 3D-printet, PLA barriere rundt isolasjonssylinderen. Overslagskanalene lå mellom barrieren og isolasjonsylinderen, som hindret økning i spenningen.

Overslagsspenningen økte svakt med prefabrikkerte NBR gummipakninger. Gummipakningene ved et rent trippelpunkt er svært følsomme for små variasjoner i plassering og form, slik at fordelen ved bruk av pakningene er liten. Simuleringene viste en tilsvarende økning i tennspenning ved riktig plassering og størrelse på pakningene.

Overslagsspenningen økte 20% med silikonpakninger støpt dirkete på testobjektet. Små variasjoner i geometrien til pakningene påvirker ikke spenningen betydelig. Tennspenningen samsvarer med hvor steamerne propagerer. Resultatene indikerer en kraftig reduksjon i feltforsterkningere rundt trippelpunktet. Det er også en økning i overslagsspenning opp til 24% ved påtrykt AC-spenning for silikonpakningene.

Table of Contents

1 Introduction

With the current environmental concerns in several industries, a need to move towards more environmentally friendly alternatives has arisen. Gas insulated switchgear (GIS) has traditionally used SF_6 as the insulating gas since it has good insulating properties. SF_6 has a global warming potential (GWP) of around 23000. This high GWP is not preferable, and new environmentally friendly gasses should be investigated as possible replacements. There is an industry preference to replace it with a gas with a similar withstand strength to maintain the dimensions of the switchgear.

A ban on PFAS materials, such as flouroketones commonly used in alternative insulation gases, is proposed by the EU [1]. Using air, probably pressurised, could be an option as an insulation gas that does not contain PFAS materials. Air does not have a high enough breakdown strength on its own, and to use air as an insulation gas some improvements should be made to reduce weak points in the insulation system. This project aims to investigate possible improvements and is limited to atmospheric air.

In GIS, a gas can never be used alone as there needs to be solid insulation materials for supports, barriers and shafts. These solid-gas interfaces are some of the weakest points in medium voltage switchgear. Understanding the streamer mechanisms along these insulation surfaces should be studied to move toward a more environmentally friendly gas. This paper is a continuation of the preliminary project where a rectangular surface profile showed to increase the breakdown strength of an insulating cylinder, and some of the results can be seen in Appendix A.1 [2].

Two main research areas are introduced in this thesis. Both aim to increase the air gap's breakdown strength with an insulating cylinder. Previous research has shown that using a dielectric barrier in rod-plane gaps can increase the breakdown strength. Part of this thesis aims to investigate whether using a barrier around the insulating cylinder can increase the breakdown strength of the solid-gas interface.

Triple junctions, where the insulation material, gas and electrode meet, are some of the weakest points in an insulation system. One possible solution to reduce the field enhancements at the triple junction is to add another insulating material at the triple junction. This thesis investigates ways to increase the inception and breakdown voltage at the weak point by adding gaskets.

1.1 Research questions

The two main research areas are divided into four research questions for the project to focus the research:

1. Can adding a dielectric barrier around an insulating cylinder increase the

breakdown strength of a solid gas interface, and how does it affect the breakdown path?

2. Will rubber gaskets at the triple junction increase the breakdown strength of an air gap with a gas-solid interface, and how do they affect streamer inception?

3. Will a silicone gasket at the triple junction increase the breakdown strength of an air gap with a gas-solid interface, and how do they affect streamer inception?

4. How do silicone gaskets affect the breakdown strength of a gas-solid interface under AC voltage?

1.2 Preliminary project

The preliminary project [2] is an unpublished work to prepare for this thesis. Part of the theory and method overlap between the two projects. The introduction, introduction, theory and method are adapted from the preliminary project, changed to correct errors, improve language and adapted to new research areas. Therefore, some parts of these sections are unchanged from the prior project, like the section on the up-and-down method. The sections about barriers and triple junctions are new to this thesis.

2 Theory

2.1 Streamer mechanism

The streamer mechanism is used to explain the pre-breakdown mechanisms in gases. Streamers are a fast-moving phenomena that create tree-like structures. When the gap distance, electric field strength or pressure is large, breakdowns are explained by the streamer mechanism. A streamer occurs when the electric field of the space charges left behind by avalanches creates an electric field comparable to the background electric field [3].

Streamers consist of an ionising front and a body of plasma filaments, as seen in figure 2.1. Depending on the polarisation of the streamer, the ionising front contains positive ions or electrons. The body of the streamer or the streamer channel is electrically neutral. The ionising front also creates a charge layer surrounding the streamer with positive charges at one end and negative charges on the other, depending on polarisation [4].

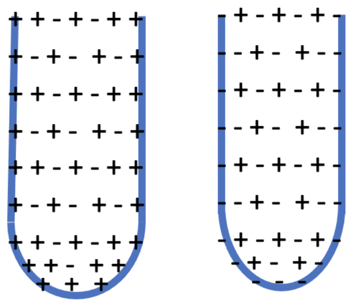

Figure 2.1: Conceptual figure of a positive and a negative streamer, the blue area is the ionising front containing positive particles or electrons, and the body is electrically neutral. Developed from [4].

Figure 2.2 shows the relation between streamer inception and propagation as a function of gap distance for a sphere-plane gap. For smaller air gaps, streamer inception will itself lead to breakdown. For larger gaps, streamer or leader propagation will also determine the breakdown strength of the gap, as seen in the figure. Streamer propagation requires a smaller electric field than streamer inception to be maintained. Leader propagation commonly only occurs for air gaps over 1m or along a dielectric surface and requires a background electric field of around $0.1 - 0.2$kV/mm for propagation. Along dielectric surfaces, leader propagation is often called a leader-like mechanism.

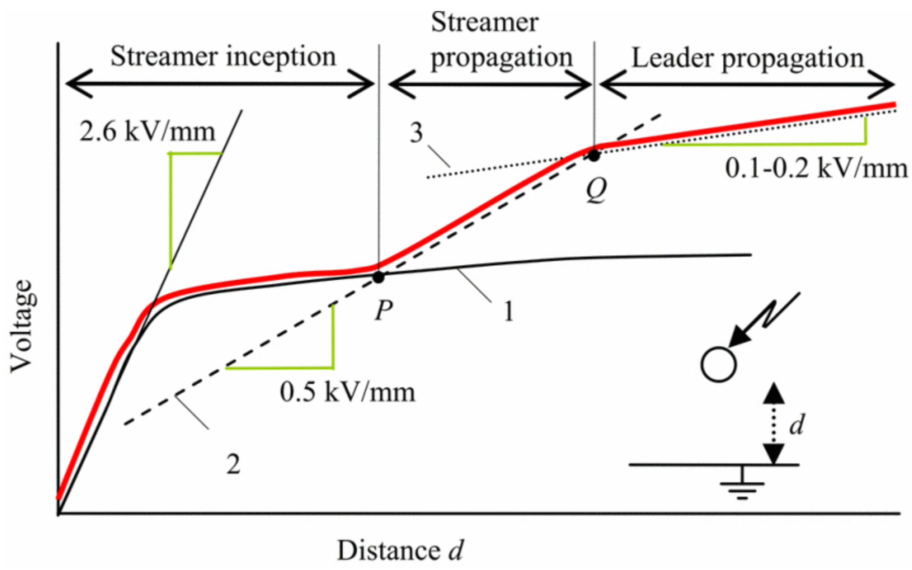

Figure 2.2: Withstand voltage U_w as a function of the gap distance for a sphere-plane gap. Figure from [5].

2.1.1 Streamer inception

For a streamer to form, an initial free electron is required. If the electric field is at a critical value, an avalanche will develop. When the critical number of electrons is generated, the streamer head will form, and streamer inception has occurred. Streamer inception follows equation (1) where Γ is the critical field line. $\alpha(|E|)$ is the field dependent ionisation coefficient, and N_{crit} is the critical number of electrons needed to form the streamer head. Inception usually occurs where the electric field strength is strongest [5].

$$\int_{\Gamma} \alpha(|E|)dx = lnN_{crit} \tag{1}$$

The streamer inception criterion is useful when designing GIS since it will ensure no breakdowns occur. Designing based only on streamer inception can be too limiting, leading to over-dimensioned GIS. There is a chance for streamer inception without breakdown, as seen in figure 2.2. Designing GIS should also be based on streamer propagation and leader propagation [6].

2.1.2 Streamer propagation

A streamer will only reach the opposite electrode if the voltage is high enough to maintain the streamer propagation. Streamer propagation does not require a high field, as the streamer is a self-sustaining mechanism [6]. The lowest possible voltage for streamer propagation is often expressed by equation (2), where d is the distance between electrodes and E_{st} is the internal field strength of the streamer. For a lightning impulse, the internal field of a positive streamer is $E_{st} \approx 0.54\text{kV/mm}$. $U_0 \approx 20 - 30\text{kV}$ is the voltage needed for the streamer to generate a breakdown [5].

$$U_w = U_0 + dE_{st} \quad (2)$$

Positive and negative streamer propagation are slightly different mechanisms affecting electron ionisation. Positive streamers are cathode-directed, and the electrons travel against the streamer propagation. The ionising front of the positive streamers consists of positive ions. Positive ions are heavier particles than electrons and move slower. Therefore, the streamer does not move because of the ions but rather ionisation in front of the streamer head. The positive streamers need free electrons from outside the avalanche to grow. Photoionisation is the most common mechanism for positive streamers to generate free electrons [4].

Photons are emitted from the positive streamer. Photons are high-energy light quanta of short wavelength. When photons collide into neutral particles, the energy can be enough for an electron to be released from the particle, leaving behind a positive ion. This process is called photoionisation.

The free electrons generated by the photoionisation can create new avalanches in front of the streamer. The electron may be accelerated towards the streamer neutralising the positive ions in the streamer head and leaving the slower positive ion behind. The accumulation of positive ions creates a positive space charge that is now the streamer head. The streamer body grows because of impact ionisation between the electron avalanche and the previous positive streamer head. This propagation can be seen in figure 2.3 [4].

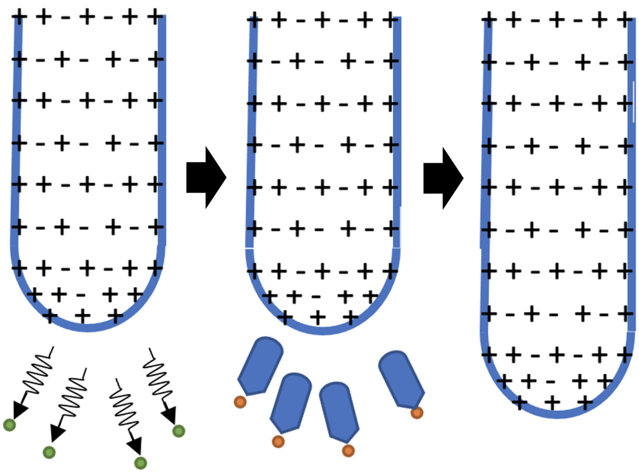

Figure 2.3: Conceptual figure of positive streamer propagation. The neutral particles are green, the positive ions are orange, and the electron avalanche is blue. Developed from [4].

Positive streamers occur easier than negative streamers. However, negative streamers can dominate when the polarity of the applied voltage is negative [3].

For negative streamers, the electrons propagate in the streamer direction. The negative streamer ionising front consists of electrons. The electrons that form the space charge around the streamer body drift away from the streamer body, decreasing the electric field caused by the streamer. Therefore, negative streamers propagate shorter than positive streamers and require a higher background field to maintain propagation [4].

Free electrons are generated by excitations, where the electron energy excites a particle. An electron is released from the particle, leading to two free electrons drifting in the streamer direction. The positive ion stays behind and becomes part of the streamer body [4].

2.2 Solid-gas interfaces in insulation systems

2.2.1 Dielectric materials in insulation systems

A dielectric material can influence the streamer mechanisms in different ways. A streamer can be attracted to the surface because of electron emission from the surface. Electron emission occurs when photoionisation bombards the dielectric surface, creating free electrons at the surface of the dielectric. Polarisation of the dielectric can also attract the particles in the gas when the relative permittivity of the dielectric is greater than the surrounding gas [6].

Surface charges will alter the electric field around a dielectric surface. A charge accumulation on the dielectric surface at the solid-gas interface will occur when the particles from previous discharges accumulate on the surface. The accumulation is commonly referred to as a surface charge [7]. These surface charges can significantly alter the electric field, potentially creating field enhancements [4].

2.2.2 Surface Profiles

From experimental results, a dielectric surface with a patterned profile, subjected to an inhomogeneous electric field, indicated that streamer propagation is reduced compared to a smooth profile. The larger surface area of the profiled pattern and the streamers propagating along the surface profiles into the corrugations are part of the explanation for this reduction [8]. The square surface profile will also increase the breakdown strength of a gas-solid interface [9].

2.2.3 The barrier effect

The barrier effect is an increase in breakdown voltage and time when a barrier of any material is placed at an optimal distance between electrodes under DC, AC, or pulsed voltages. The barrier effect is commonly observed in rod-plane gaps when a dielectric is placed in the gap. The optimal position of the dielectric barrier is at $15 - 30\%$ of the gap from the rod. The breakdown strength is observed to increase up to 3 times depending on the gap and polarity [10].

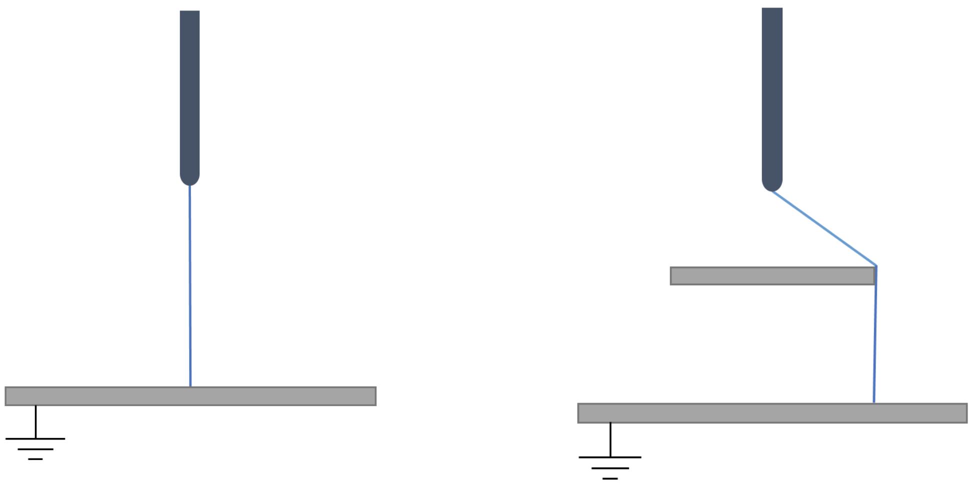

(a) *Shortest streamer path without a barrier.* (b) *Shortest streamer path with a barrier.*

Figure 2.4: Figure of the shortest streamer path for a rod-plane gap with and without a barrier. Developed from [6].

When the streamers don't cause a puncture in the barrier, it can increase the shortest streamer path by leading the streamer to propagate around the barrier, as seen in figure 2.4 [6]. The increase in streamer path increases the withstand voltage related to streamer propagation.

A barrier surrounding a cylinder has previously been shown to create a slow path and a fast path for streamers to propagate. The fast past is along the insulating cylinder and is faster due to the insulating material. The barrier can cut off the fast path. The slow path, similar to the path in figure 2.4b, would reach the cathode first. A higher electric field was required for breakdown to occur [11].

Ionisation occurs near the needle tip. For a positive gap, the electron drift leads to electrons moving towards and recombining at the needle tip. The positive ions are left behind. These positive particles will move towards the negative electrode and accumulate on the barrier, weakening the electric field between the barrier, and the breakdown strength increases [10].

2.2.4 Triple junctions

Intersections between metallic conductors, the solid insulating material, and the surrounding gas are referred to as triple junctions. Triple junctions are one of the weakest points in gas insulated systems and are commonly where streamer inception occurs. The influences of the dielectric material create local field enhancements close to the electrode, where streamers often initiate. A charge transfer between the electrode and the dielectric also occurs to generate a charge equilibrium. This charge transfer leads to a difference in surface potential, further contributing to the distortion of the electric field at the triple junction [12].

2.3 Atmospheric conditions in air

When testing in atmospheric air, the breakdown voltage is disrupted by the temperature, pressure, and humidity. The withstand strength is increased with increasing density or humidity unless there is condensation. When the relative humidity exceeds 80%, the withstand strength becomes irregular. Therefore, the breakdown strength should be corrected using the correction factors for atmospheric air. The standard conditions are $t_0 = 20°\mathrm{C}$, $p_0 = 101.3\mathrm{kPa}$ and $h_0 = 11\mathrm{g/m}^3$ [3].

To correct for atmospheric conditions, the two correction factors k_1 and k_2 are used as seen in equation (3).

$$U = k_1 k_2 U_0 \tag{3}$$

The correction factor k_1 is the correction factor for air density, which can be found using equations (4) and (5) [3].

$$k_1 = \delta^m \tag{4}$$

$$\delta = \frac{p}{p_0}\frac{t_0}{t} \tag{5}$$

where t and t_0 are in $°K$.

For many air gaps $k_2 = 1$, only the correction factor for air density is used. When this occurs, m is always 1, leading to equation (6).

$$U = \delta U_0 \tag{6}$$

3 Method

3.1 Test object

The test object consists of two base toroids spaced 6cm apart by an insulating cylinder as in figure 3.1. One base toroid is connected to ground, the other to the impulse generator. Three different geometries are used for the electrode connected to ground, an asymmetrical sharp edge, a symmetrical sharp edge and a pure triple junction seen in figure 3.3. Both sharp edges have an edge with a thickness and height of 2.5mm protruding out of the base toroid close to the centre. The sharp edge promotes the inception of streamers. At the other base toroid, a toroidal half circle with a radius of 9mm creates the electrode connected to the voltage source seen in figure 3.2a. This circle is centred around the dielectric material with a total outer radius of 35.5mm.

There is a chance of measuring errors from changing the parts of the test object, leading to possible variations in the distance between electrodes and the centring of the cylinder.

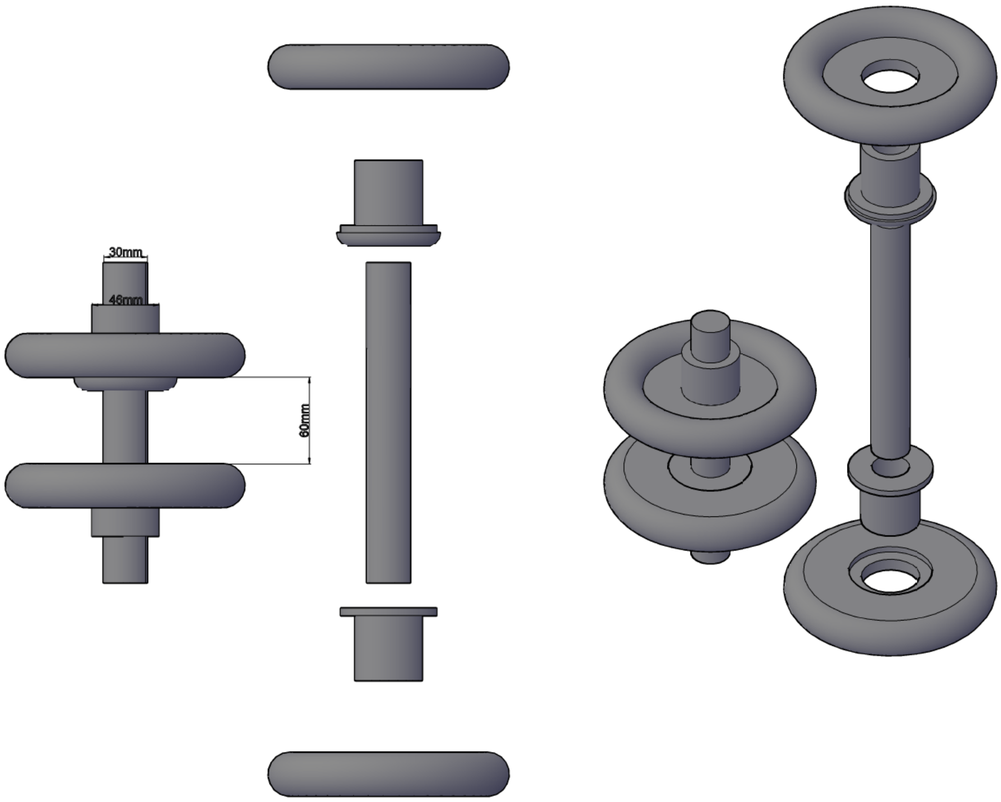

Figure 3.1: CAD images of the test object created in AutoCAD.

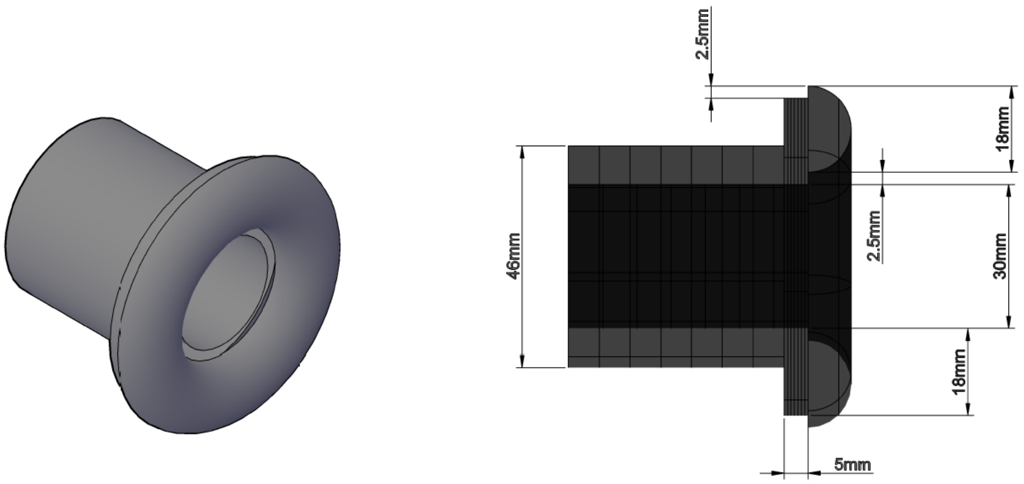

(a) *Dimensions of the electrode on the other side.*

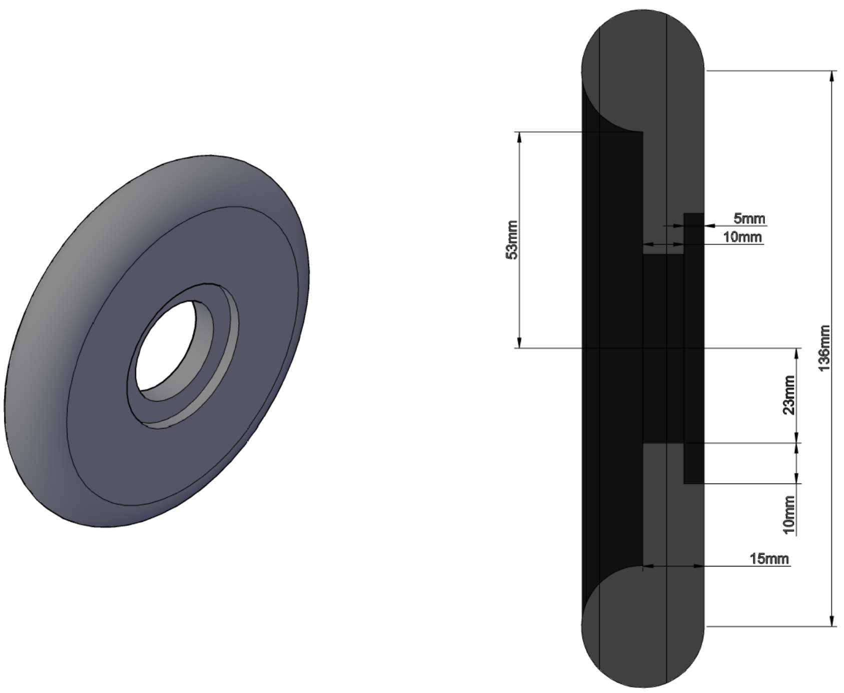

(b) *Dimensions of the toroid.*

Figure 3.2: CAD images and dimensions of the test object created in AutoCAD.

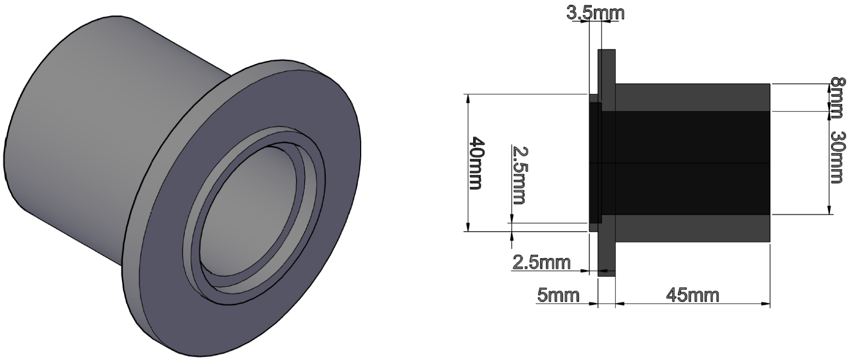

(a) Dimensions of the electrode with a symmetrical sharp edge.

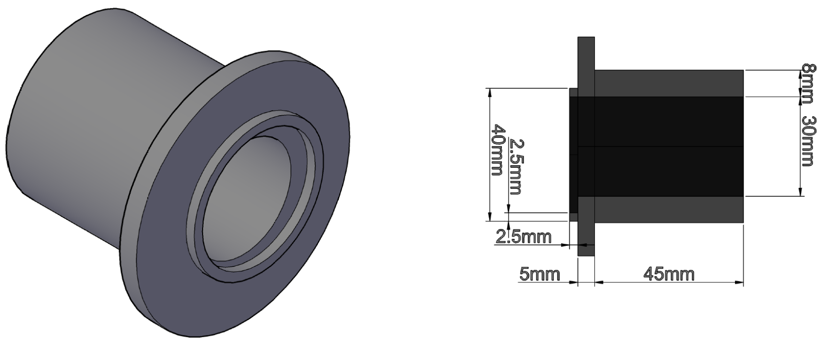

(b) Dimensions of the electrode with an asymmetrical sharp edge.

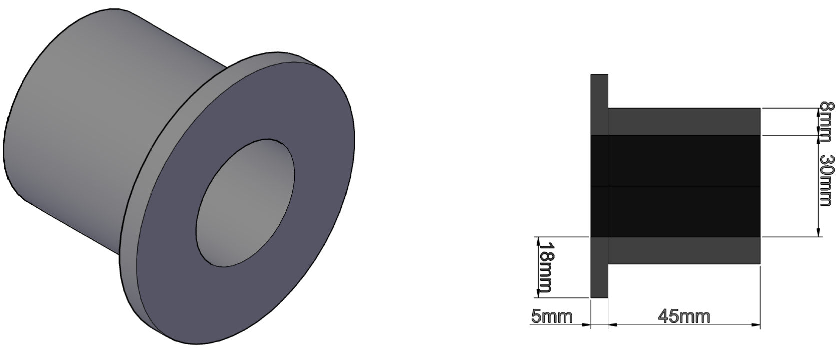

(c) Dimensions of the electrode with a pure triple junction.

Figure 3.3: CAD images and dimensions of the electrode geometry created in AutoCAD.

Two insulating cylinders are used. A cylindrical insulating rod made of polyoxymethylene (POM) reinforced with 25% glass fibres, with a relative permittivity $\epsilon_r = 3.8$ and a diameter of 29.5mm, is placed between the two electrodes. The second cylindrical insulating rod is made of polyoxymethylene (POM) and is not reinforced with fibreglass, with a relative permittivity $\epsilon_r = 4.1$ and a diameter of 29.5mm. The insulating cylinders have two different profiles; smooth and square-patterned. The square surface profile has 0.5mm deep rectangular corrugations around the insulating cylinders. The dimensions of the surface profiles are shown in figure 3.4.

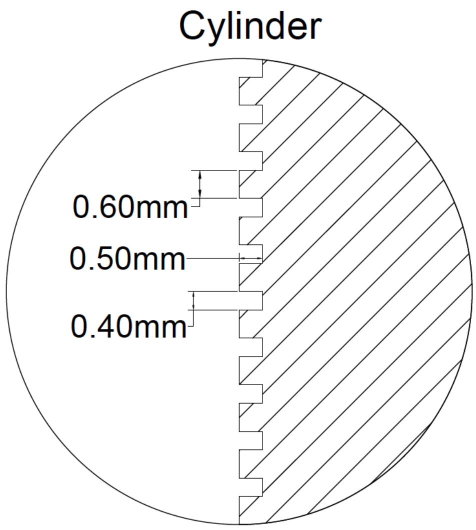

Figure 3.4: Conceptual image of the surface of the square insulator cylinder, some error is expected in the dimensions.

3.1.1 Barriers around the insulating cylinder

Barriers are made to test if the barriers can be implemented in combination with the solid-gas interface to increase the breakdown strength. This is done by placing a rounded barrier around the insulating cylinder. Two prototypes of the barriers with different dimensions are made. The barriers are 3D printed in PLA with a 0.4mm nozzle and 0.1mm layer height in an Ultimaker S5 3D printer. The infill of the printer is set to 100%, meaning the barrier is entirely solid.

The prototypes have a neck surrounding the insulation cylinder and a barrier part as seen in figure 3.5 and 3.7. The inside of the neck has a surface pattern of 0.85mm, 0.75mm and 1mm, as seen in figure 3.6, in an attempt to stop the streamers from propagating on the inside of the barrier. The barrier plate has the same surface pattern on the side facing the electrode with the sharp edge where the streamer inception occurs. The prototypes are printed in four parts. The neck and barrier plate are glued together to create two sides of the barrier. Due to human error in the glueing process, the parts do not fit together perfectly. The two sides are then screwed together around the profiled cylinder using nylon screws. The profiled cylinder is used since the barriers are easier to place with the profiled cylinder and as an attempt to further reduce the streamers propagating on the inside of the barrier neck. The POM-cylinder with fibreglass was used for the first prototype. The POM-cylinder without fibreglass was used for the second. This cylinder had a lower breakdown voltage when comparing results for the up-and-down test to a reference without the barrier. Therefore, the two prototypes are compared to the corresponding cylindrical reference.

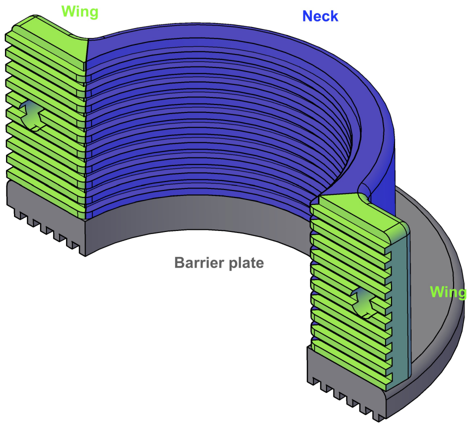

Figure 3.5: Image of the second prototype of the barrier, showing the different areas of the prototype.

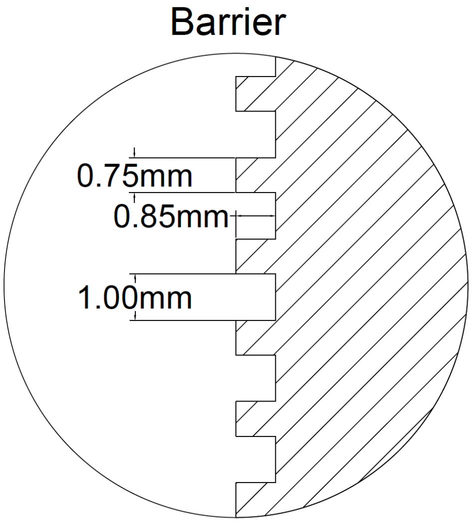

Figure 3.6: Conceptual image of the surface of the square barriers, some error is to be expected in the dimensions.

There are slight differences between the two prototypes illustrated in figure 3.7. The first barrier has a 21mm wide plate and a 30mm internal diameter. The second barrier has a 10.5mm plate and an internal diameter of 29.8mm, as it was discovered that the insulating cylinder was slightly smaller than expected. The plate was smaller in the second prototype to test if a smaller plate resisting the streamers would increase the chance of streamers propagating around the barrier. The wings of the barrier were changed to reduce the streamer propagation along the wings. The placement of the barriers was also changed. Prototype 1 was placed 1.8cm up from the base electrode. Prototype 2 was placed 1cm above the base electrode.

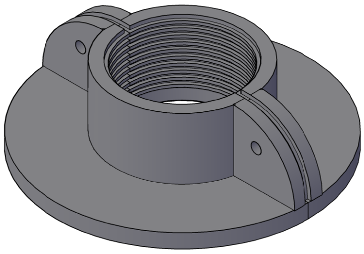

(a) Prototype 1 of the barrier.

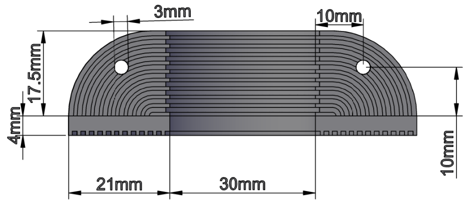

(b) Half of prototype 1 with dimensions.

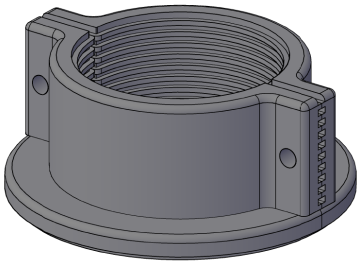

(c) Prototype 2 of the barrier.

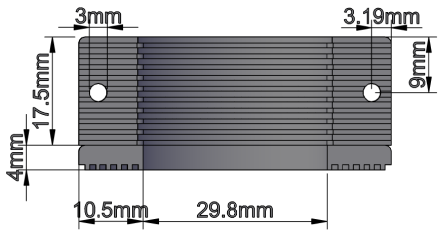

(d) Half of prototype 2 with dimensions.

Figure 3.7: CAD images of the two barrier prototypes.

From testing the barriers with the up-and-down test, it was observed that the nylon screws holding the two parts together are the weakest point in the barrier, seen in figure 3.8. Any test where the screws broke or the barrier was not fully intact after a test was rejected. For the small barrier, prototype 2, made to fit the insulating rod better, an up-and-down test could not be completed without the screws breaking. Strips were instead used to hold the barrier in place. The strips were not as tight around the insulating cylinder.

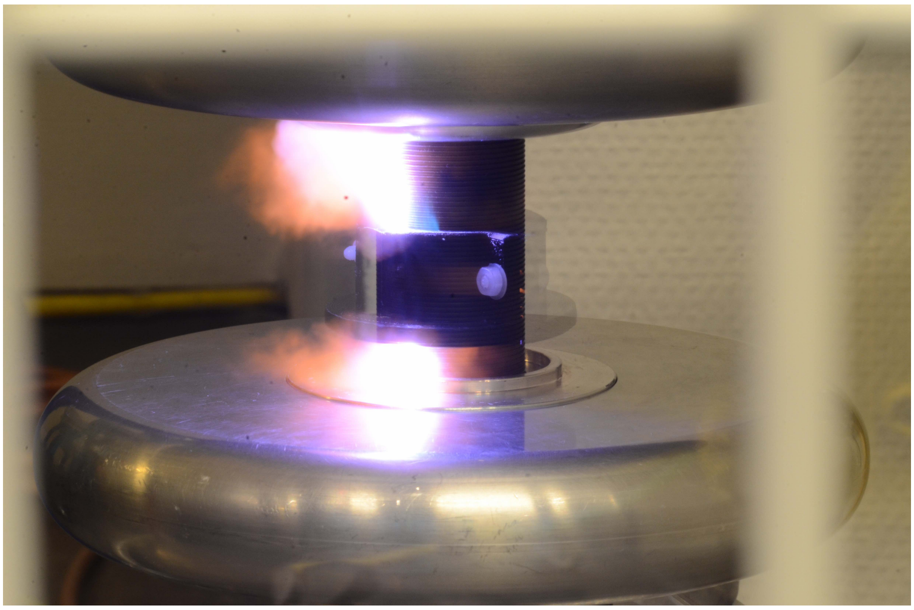

Figure 3.8: Barrier prototype where the screw is broken during breakdown. The barrier is positioned 1cm up from the toroid.

3.1.2 Gaskets at the triple junction

Triple junction gaskets are made in an attempt to increase the breakdown and inception voltage at the triple junction. There are two main reasons for using the gaskets. The first is creating an even gap distance between the insulating cylinder and the triple junction electrode. As seen in figure 3.9, the gap distance plays a large part in the inception voltage, and the cylinder being off-centre could lead to inception occurring at a lower voltage. Part of the COMSOl model used to find this inception voltage can be seen in figure 3.10. The other reason is that adding a material at the intersection between the electrode and the insulating cylinder is that it can reduce the field enhancements at the triple junctions. The gasket can also act as if there is no gap at the triple junction, by filling the gap with the gasket, which has the highest inception voltage until 3mm gaps.

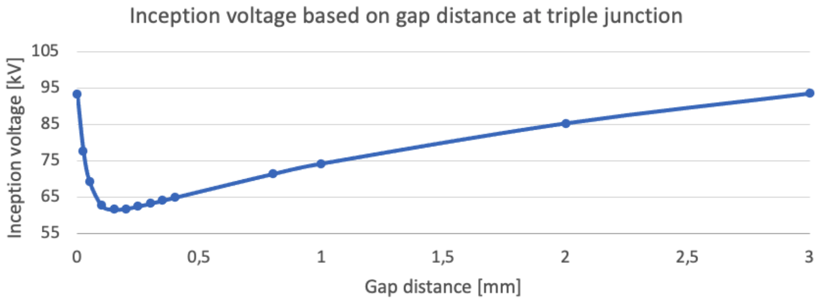

Figure 3.9: A graph of the inception voltage as a function of the gap distance between the insulating cylinder and electrode. Inception voltages are found using COMSOL and inception voltage script as described in section 3.4. The electrode has a constant inner radius of 15mm, while the insulating cylinder radius is changed to increase the gap distance. The cylinder has permittivity $\epsilon_r = 4.1$.

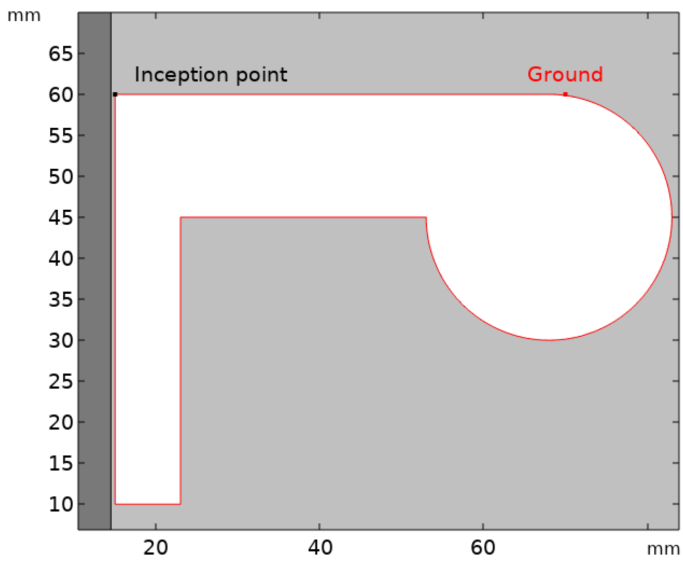

Figure 3.10: The COMSOL model of the ground electrode for simulating the inception voltage as a function of the gap distance. The inception point is where the streamlines used to calculate the inception voltage are initiated. The gap distance is 0.5mm *and the cylinder has a radius of* 14.5mm*.*

Several gaskets are made, and three of them can be seen in figure 3.11. There are rubber gaskets with $\epsilon_r = 10.8$ and silicone gaskets with $\epsilon_r = 2.9$. The rubber gaskets are rounded O-rings and a square gasket placed in milled slots in the insulating cylinder. The silicone gaskets have different amounts of silicone and are cast directly on the test object.

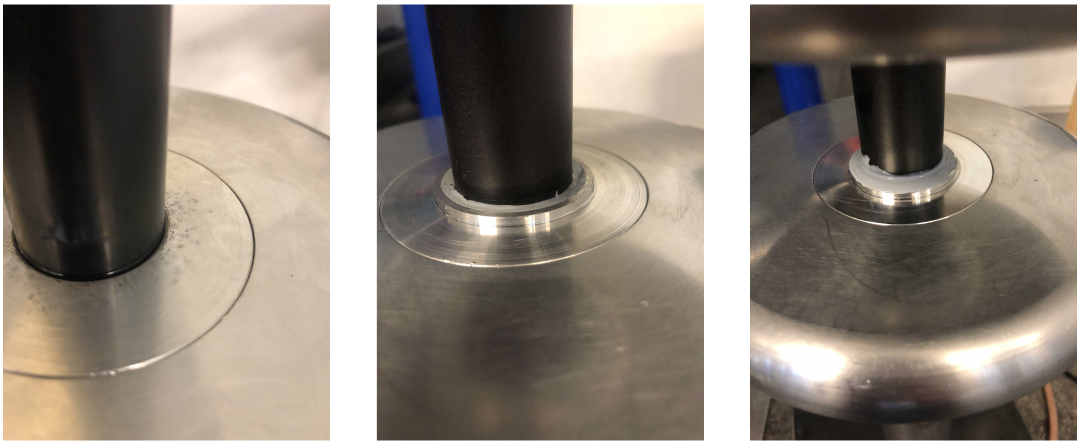

(a) O-ring gasket. *(b) The first silicone gasket.* *(c) The second silicone gasket.*

Figure 3.11: Images of three gaskets with the electrode and insulating cylinder.

Both rubber gaskets are added by milling two 3mm slots 1cm apart in the insulating cylinders for the rubber gaskets to slot into. Grease was added to the cylinder after the slots were milled for simpler application of the gasket and gradually removed throughout the tests. The rubber gaskets are tested with the pure triple junction as the electrode. The O-rings are made of Perbunan, a Nitrile butadiene rubber. They are tested in three different sizes, seen in table 3.1. The top O-rings are placed at the intersection of the cylinder and metal electrode so that the largest point of the gasket touches the intersection. The bottom O-rings, except for O-ring 2, are placed further down in an attempt to centre the cylinder. The square gasket is cut out of rubber and placed in the top milled slot to exactly fit the slot and the gap. A grease is used to manoeuvre the gasket and cylinder into the electrode. The square gasket is placed so the top of the gasket is at the intersection. The reference test without a gasket is completed using the same cylinder, placing the milled slots approximately 1cm into the triple junction.

Table 3.1: Dimensions of the three O-rings.

O-ring 1	18.72x2.62mm
O-ring 2	20.22x3.53mm
O-ring 3	20x3mm

The silicon gaskets are created with a symmetrical sharp edge. To fill in the entire gap between the insulating cylinder and the electrode, the sharp edge is filled to the brim with POWERSIL® XLR® 630 A/B silicone [13]. The two-part silicone is combined and poured between the cylinder and electrode. Then it is heated to 105°C in a heating chamber with the cylinder and electrode. When the silicone has been heated and cooled, the overflowing silicone is cut off for the first silicone gasket, and any excess that has spilt over the sharp edge is removed for the second silicone gasket.

3.2 Lightning impulse testing

This section explains the experimental setup and method used for the lightning impulse testing for both barriers and triple junction gaskets.

3.2.1 Experimental setup

The measuring circuit consists of a 200kV impulse generator and the test object. The circuit can be seen in figure 3.12 and 3.13. The oscilloscope is connected using a North Star PVM-100 probe with a 1 : 2000 divider ratio and maximum measuring voltage of 150kV [14].

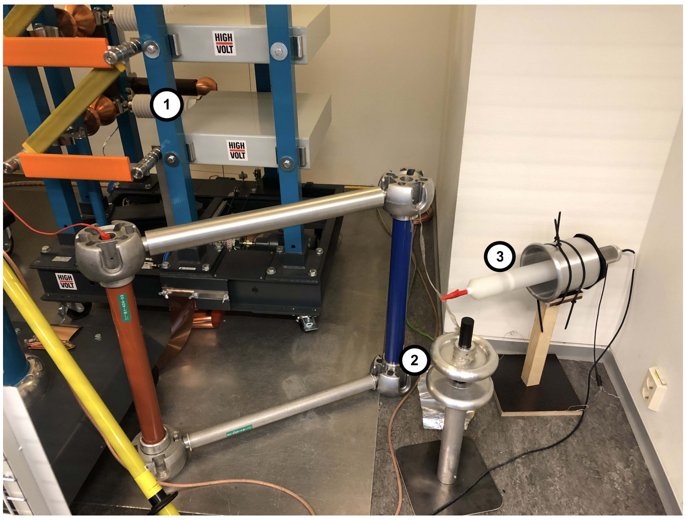

Figure 3.12: Image of the experimental setup. 1) Impulse generator. 2) Test object. 3) Measuring probe.

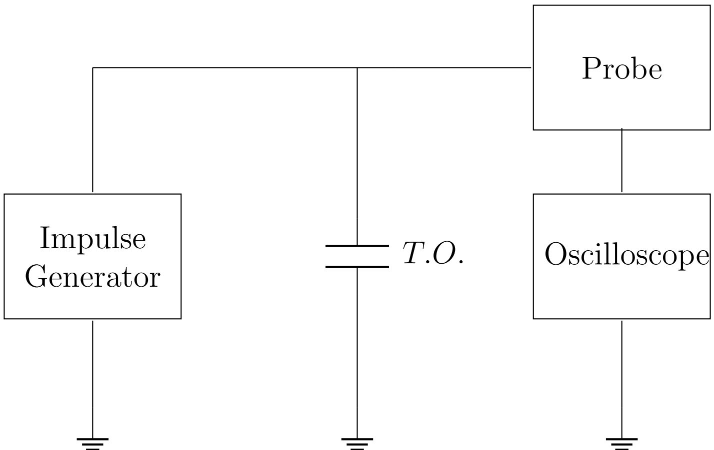

Figure 3.13: Schematic drawing of the experimental setup. T.O. is the test object.

3.2.2 Impulse generator

An impulse generator with two stages is used, implementing both stages to get impulse voltages up to 200kV. The values for the impulse generator are seen in table 3.2.

Table 3.2: Values for the impulse generator for each stage [15].

Component	Value
R_d - Damping resistance	43 Ω
R_e - Discharge resistance	132 Ω
C_s - Charging capacitance	500 nF

The impulse generator generates the standard lightning impulse (LI) 1.2/50µs with a 30% tolerance for the front time and a 20% tolerance for the time to half value, as shown in figure 3.14 according to IEC 60060-1 [16].

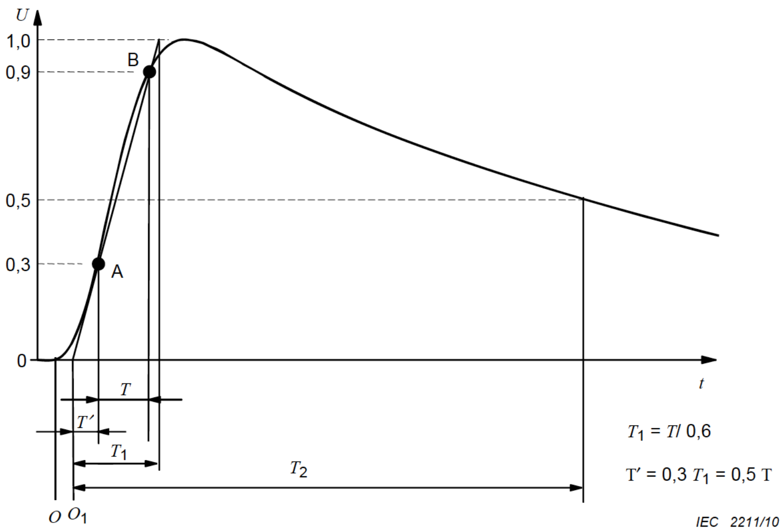

Figure 3.14: Lightning impulse as a function of voltage and time [16].

The actual recorded LI in figure 3.15 confirms that the front and half times are within the tolerated range. The polarity of the LI is arbitrary for finding the front and half time. Still, only negative LIs are used in this thesis since negative impulses at the top electrode are the most critical for this test object. The front time is of the relation $T_1 = T/0,6 \approx 1.67T$, where the 60% rise time is recorded. The front time of recorded LIs is about $T_1 = 1.67 * 800\text{ns} = 1.34\mu\text{s}$. This is within the tolerated range. The half time, $T_2 = 46.5\mu\text{s}$, is also within the tolerated range.

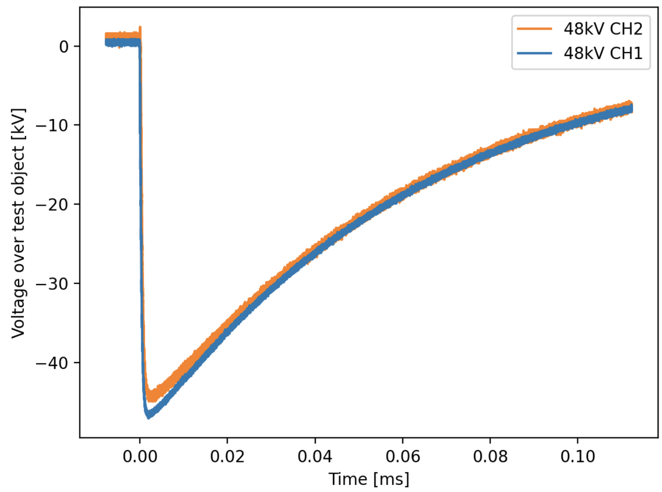

Figure 3.15: Lightning impulse with 48kV charging voltage. Channel 1 is measured over the test object using a probe, and channel 2 is measured using the measuring circuit and a voltage ratio of 1 : 24890. $U_{peak} = 47.9492kV$ at channel 1 and $U_{peak} = 47.1052kV$ at channel 2.

The ratio between the charging voltage and the voltage over the test object is measured and used as a voltage ratio for the breakdown voltage. There is a ratio of 0.9989 from the charging voltage set on the impulse generator to the voltage measured over the test object with the probe. The probe is represented at channel 1. The voltage probe has an accuracy of 2% for frequencies in the range of the LI from 200Hz-5MHz [14]. Channel 2 is measured using a measuring circuit over the voltage divider of the impulse generator [17]. This measuring circuit has previously been tested for a voltage ratio of 1 : 24890, while this gives a slightly smaller voltage measured voltage and a ratio of 0.9813 compared to the charging voltage. The ratio is measured as the peak-peak value in figure 3.15 and includes a small dip in the voltage as the LI starts.

Although the voltage probe is not fully accurate, the placement closer to the test object and the slightly more precise waveform, without the dip in voltage, makes it more reliable for measurements. The ratio from the probe is used to estimate the actual voltage over the test object. Some variations between the LIs are to be expected and are a source of error.

3.2.3 Camera

Since streamers and leaders are fast phenomena, cameras are needed to see them. For this project, a Nikon camera with a 1.3s shutter speed and an aperture of 32 is used to capture the breakdown channels. The big shutter time, the manual trigger for the LI, and a remote trigger for the camera ensure that the breakdown channels are captured in the photos. The camera is placed outside of the high voltage cell for protection of the camera and ease of access. This leads to the grid from the cell wall being visible and slight reflections in the Plexiglas of the cell wall disturbing the image.

3.2.4 Up-and-down method

The up-and-down method is a systematic approach to get the 50% breakdown voltage, U_{50} when applying a LI as described in IEC 60060-1 [16].

When completing an up-and-down test, the lowest voltage for breakdown must be estimated, as well as the voltage step size, ΔU. The lowest voltage can be difficult to find and is based on an educated guess. The voltage step size should be chosen as $\Delta U \approx 1.5\% - 3\% U_{50}$ for the approximate value of the 50% breakdown voltage and is an educated guess based on the estimated breakdown voltage.

A voltage sufficiently below the approximated lowest voltage for breakdown is chosen and is the same for all up-and-down tests completed in this thesis. Before a breakdown occurs the voltage step can be slightly higher than ΔU. For this project $\Delta U = 1$kV charging voltage is used after the first breakdown and $\Delta U = 4$kV is used before the first breakdown. The voltage is increased or decreased with ΔU depending on whether a withstand occurs. If a withstand occurs the voltage is increased and if not it is decreased, following a curve like the one in figure 3.16.

According to IEC 60060 a minimum of 20 LIs should be completed from the first breakdown [16]. In this project, 20 LIs are chosen as the standard test number but can be increased if deemed necessary due to the large standard deviation.

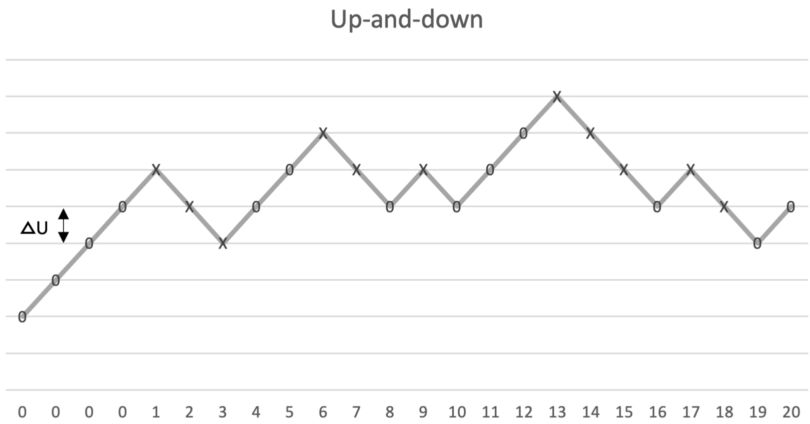

Figure 3.16: Example of an up-and-down test, where 0 indicates a withstand and X a breakdown.

The 50% breakdown voltage can be calculated using equation (7).

$$U_{50\%} = U_0 + \Delta U \left(\frac{A}{k} - \frac{1}{2} \right) \tag{7}$$

where $A = \Sigma i k_i$ and k_i is the number of breakdowns at each voltage level i from ΔU and k is the total number of breakdowns [18]. U_{50} is corrected for atmospheric conditions and the ratio of voltage over the test object.

The standard deviation requires multiple tests to be accurate, meaning that estimates need to be used to get precise results when only a few impulses are tested. The estimate of the standard deviation for up-and-down testing can be found using (8)

$$\sigma_{est} = 1.62 \Delta u \left(\frac{kB - A^2}{k^2} + 0.029 \right) \tag{8}$$

where $A = \Sigma i k_i$ and $B = \Sigma i^2 k_i$, k_i is the number of breakdowns at each voltage level i from ΔU and k is the total number of breakdowns [18].

A previous discharge can affect the results of the up-and-down test. To reduce this effect, a one minute wait between each LI is applied.

3.3 AC testing

For the silicone gaskets, it is beneficial to get an understanding of the breakdown voltage during AC to understand if they can be used during normal operation.

3.3.1 Experimental setup

The AC circuit consists of a 220V/100kV transformer and a variable autotransformer (variac), a water resistance and the test object as seen in figure 3.17. The voltage is measured on the low voltage side of the transformer using a P5200A Series High Voltage Differential Probe with a 500 : 1 ratio connected to the oscilloscope [19]. From testing with a probe over the test object, the voltage ratio was confirmed to be 232000 : 1 on the oscilloscope. The current is measured on the low voltage side using a current loop scaled to 1 : 100mA. The current is used to capture the waveform on the oscilloscope during breakdown, since the current increases during a breakdown. The trigger level is set to around 3A.

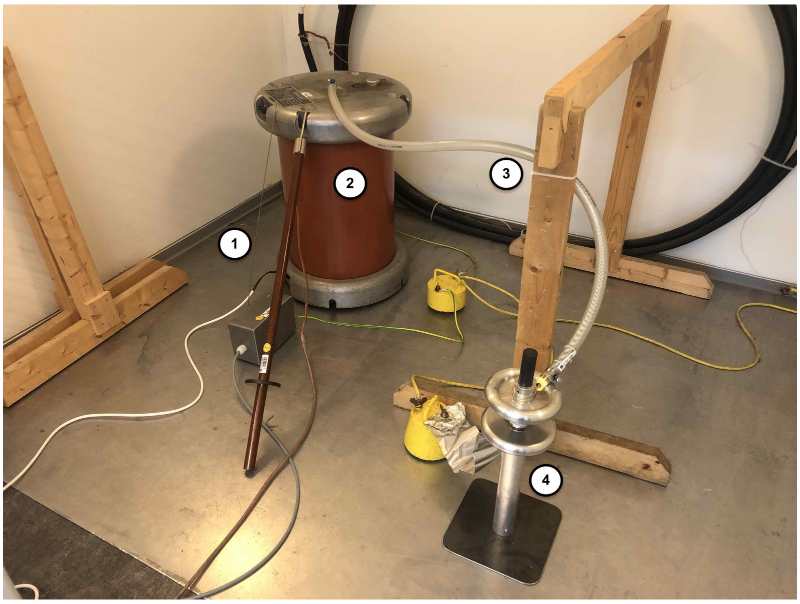

Figure 3.17: Image of the experimental setup for AC testing. 1) Grounding knife and rod. 2) Transformer. 3) Water resistance. 4) Test object.

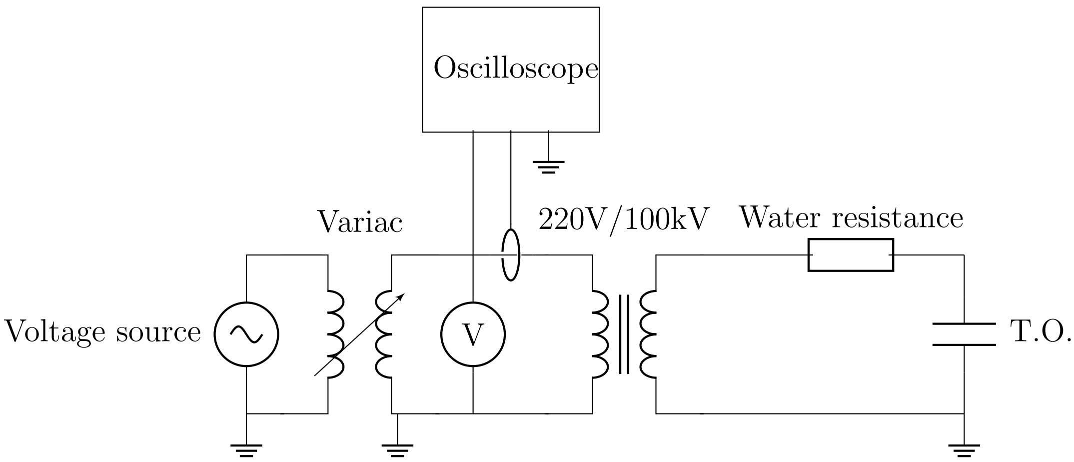

Figure 3.18: Test setup for AC testing. Current and voltage are measured on the low voltage side. Current using a current loop, while the voltage is measured using the variacs internal voltmeter connectred to a probe.

3.3.2 Breakdown voltage

A rising voltage test is used to find the breakdown voltage of the test object when AC voltage is applied. The test method is a continuous method, where the voltage is applied gradually until breakdown occurs. Once breakdown occurs the breakdown voltage is found using peak-peak measurements on the oscilloscope and converted to RMS values. The voltage is then adjusted to atmospheric conditions. This procedure is repeated five times for each test to get an average breakdown voltage. A one minute wait between each test is used.

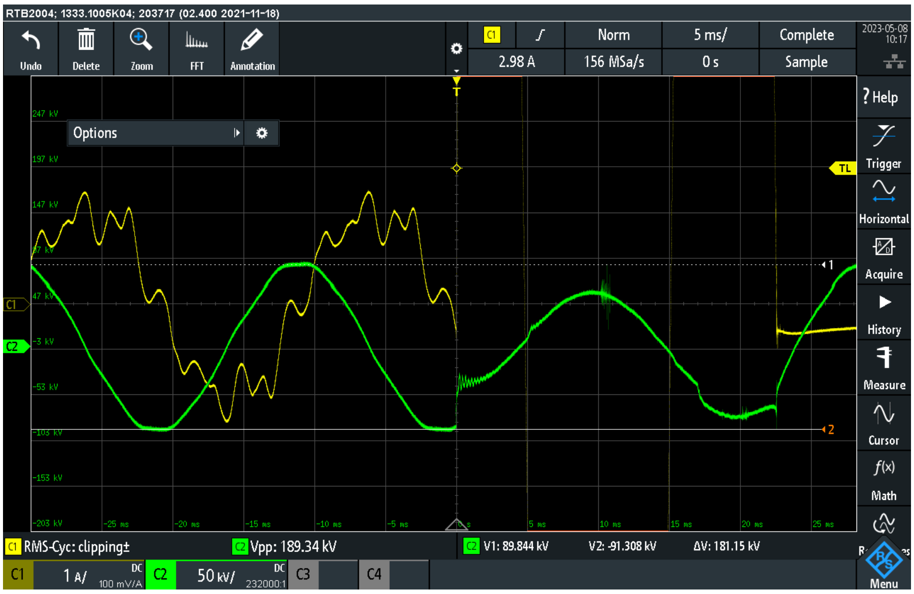

Figure 3.19: Breakdown during AC test. Breakdown during the negative half period. Channel 1 measures the current, since the voltage was rising, there was noise on the current. Channel 2 measures the voltage. The peak-peak value is measured with cursors before breakdown.

3.4 Electrostatic simulations

To investigate the breakdown phenomena that occur with the gaskets and barriers, a model of the test object is created in the finite element modelling (FEM) tool COMSOL. The modelling is limited to stationary electrostatics. A 2D-axial symmetrical model of the test object approximates the 3D geometry. The model consists of the two electrode geometries, the insulating cylinder, the gaskets and the surrounding air seen in figure 3.20. The boundary at the outer edge is set to zero charge. The electric potential is placed around the top electrode. Ground is set to surround the bottom electrode.

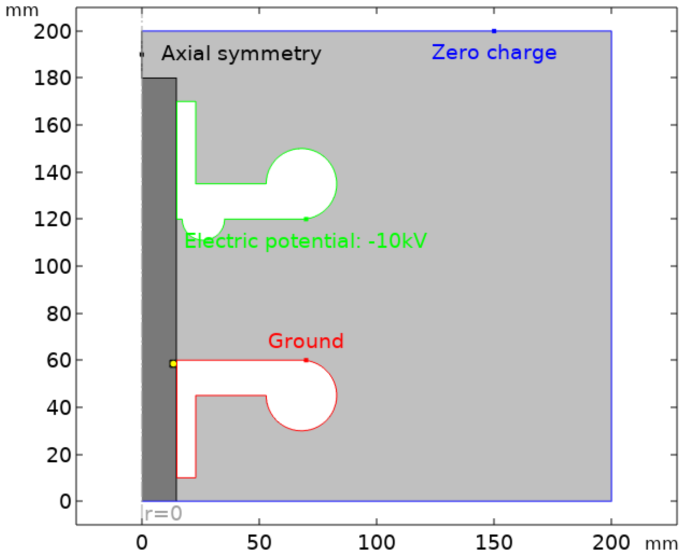

Figure 3.20: The geometry of the COMSOL model with O-ring 3. The cylinder is dark grey, the air is light grey and O-ring 3 is yellow.

The mesh is physics-controlled and extremely fine, as seen in figure 3.21, to capture the details of the geometry around the inception point.

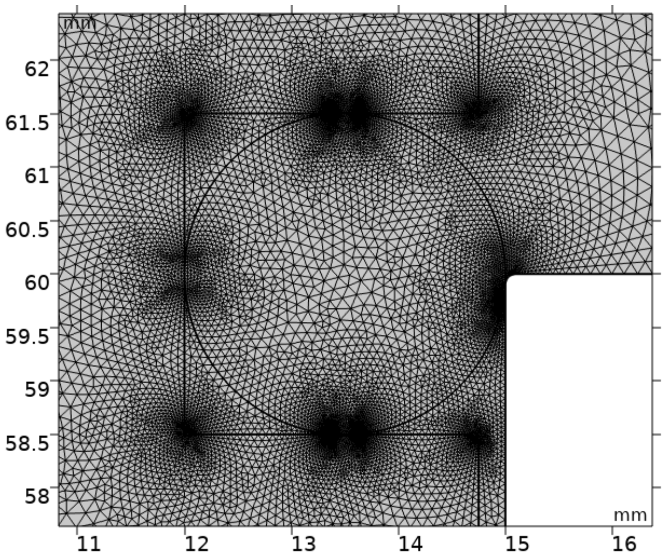

Figure 3.21: A figure of O-ring 3 in a COMSOL model with the mesh.

The barriers are tested with the geometry of prototype 2. The sharp edge used is the asymmetrical sharp edge, and the simulations are computed with a sharp edge at 0.5mm from the edge. The barrier is placed 0mm from the gap, with dimensions of the intersection of the prototype. The relative permittivity of the barrier is chosen as 2.675 from the preset values of acrylic plastic in COMSOL. The cylinder is profiled and has $\epsilon_r = 4.1$.

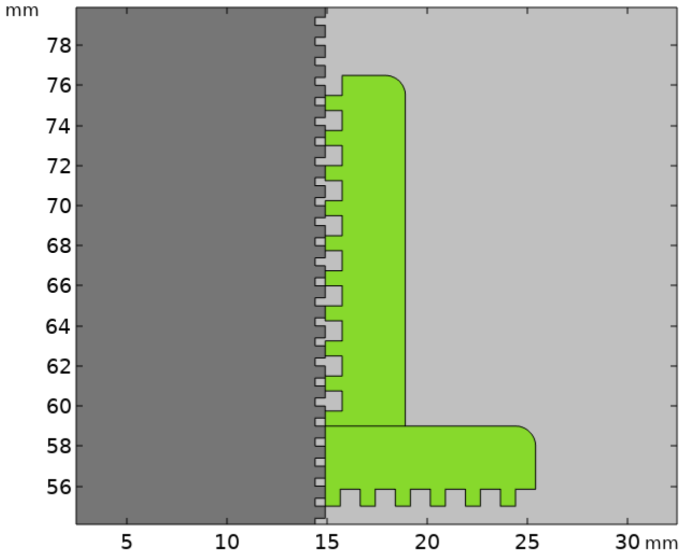

Figure 3.22: The geometry of the COMSOL model with prototype 2 as a barrier.

Since a few different gaskets are tested, the different geometries are simulated. The rubber gasket geometry can be seen in figure 3.23a for O-ring 3, where the gasket is simulated with a pure triple junction. The placement of the gasket is defined using a neutral point, where the top of the gasket is at the same level as the top of the electrode. The rubber gaskets are simulated using the permittivity for pure Nitrile butadiene rubber at $\epsilon_r = 10.8$ [20]. The cylinder has a relative permittivity of 4.1.

O-ring 1 and 2 are simulated with a few variations on the geometry of O-ring 3. The size is changed and made to fit the milled slot. For O-ring 1, the gasket is placed in the bottom left corner of the milled slot. O-ring 2 is positioned as far into the slot as possible. The square gasket is placed at the neutral point and has the same geometry as O-ring 3, where the radius of the corners is 0.1mm, so it fills the milled slot as seen in figure 3.23b.

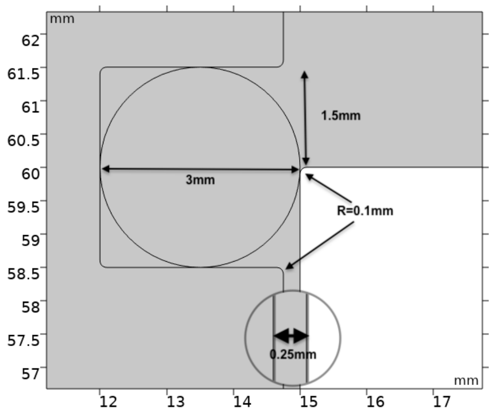

(a) Dimensions of O-ring 3 used in simulations, placed 1.5mm up form neutral position.

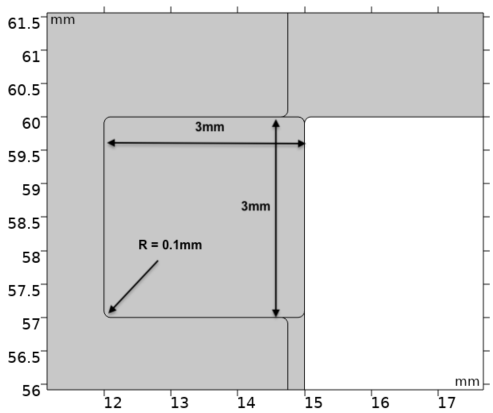

(b) Dimensions of the square gasket used in simulations, placed at the neutral position.

Figure 3.23: Dimensions of the rubber gaskets used in COMSOL simulations.

Figure 3.24 shows the dimensions of the second silicone gasket with overhanging silicone simulated with a symmetrical sharp edge. The overhanging part of the silicone is simplified to a 0.1mm layer above the sharp edge. All edges are rounded with a radius of 0.1mm. For the gasket without overhanging silicone, the silicone is 0.1mm shorter and rounded with a radius of 0.1mm at the junction between the sharp edge and the silicone. The silicone is simulated with $\epsilon_r = 2.9$. The insulating cylinder has a relative permittivity of 3.8.

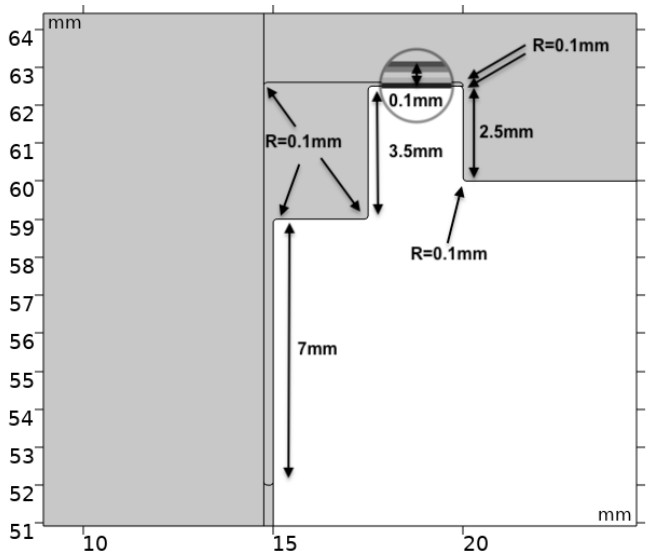

Figure 3.24: Dimensions of the second silicone gasket with overhanging silicone.

3.4.1 Inception voltage

The inception voltage is found using a Python script developed by Hans Kristian Hygen Meyer. The script can be seen in Appendix B.2. The streamer inception equation (1) is used. The electric field is incrementally increased until the integral is equal to or larger than lnN_c. When this criterion is achieved, the voltage is the lowest voltage where inception can occur. $lnN_c = 9.15$ for simulations in air. The applied voltage in the simulations is -10kV at the upper electrode, and the pressure is 1bar. Field lines are the streamlines exported from the COMSOL simulations. The streamlines, in the gas phase, are taken from the edge of the triple junction as seen in figure 3.25 or the sharp edge for most tests, where the electric field is the highest. The streamlines are in kV/mm.

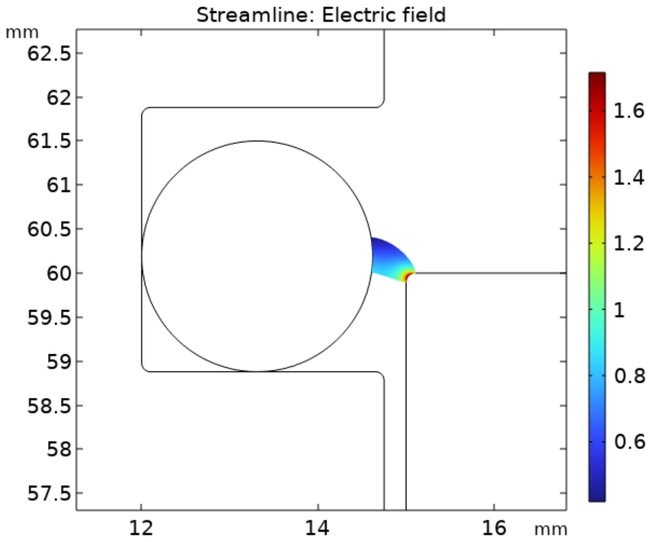

Figure 3.25: A figure of the streamlines in air with an E-field in kV/mm. Here with O-ring 1, at the 1.5*mm placement.*

The script uses Petcharacks equations for air to find $\alpha(|E|)$ along the streamline [21]. These equations can be seen in Appendix B.1.

α/p is integrated starting at the electrode where $\alpha > 0$ and ends at $\alpha = 0$. If the integral is lower than the streamer constant, the electric field is scaled up, and the integral is computed again. The voltage is linearly scaled along with the electric field. The voltage, when the streamer inception equation is fulfilled, is the inception voltage.

4 Results and Discussion

4.1 Barriers

This section aims to answer the first research question regarding whether using a barrier could increase the breakdown strength of the air gap with a solid-gas interface.

The 2 prototypes in figure 3.7 are placed around the insulating cylinder. Both POM-cylinders with and without fibreglass are used in this section and the reference voltages are based on this difference. The profiled insulating cylinders are used with an asymmetrical sharp edge as the electrode. Up-and-down tests are completed to find the 50% breakdown voltage. Multiple tests were completed, while only three tests were completed without the barriers breaking.

Table 4.1: 50% breakdown voltage of both barrier prototypes compared to the reference voltage with the corresponding insulating cylinder. Only tests where the barriers are intact at the end of the test are included.

	U_{50} [kV]	σ_{est} [kV]	Reference U_{50} [kV]
Prototype 1 Test 1	95.05	5.47	91.13
Prototype 1 Test 2	91.04	2.98	91.13
Prototype 2	67.45	10.17	68.35

As seen in table 4.1, there is an increase in the breakdown voltage for the first test for prototype 1 compared to the second test. The increase is within the standard deviations of the tests and is deemed insignificant, but the two tests for prototype 1 were completed right after one another, only shifting the placement of the entire test object, which should not affect the tests. There are some natural variations in the breakdown voltage related to the stochastic nature of breakdowns, however, the difference is quite large. As seen in figure 4.1, there is a gradual increase in the breakdown voltage during the first test leading to a larger estimated standard deviation. The cylinders and barriers were not cleaned for surface charges, and there was likely an accumulation of surface charges affecting the tests. The surface charges were not measured and are not certain.

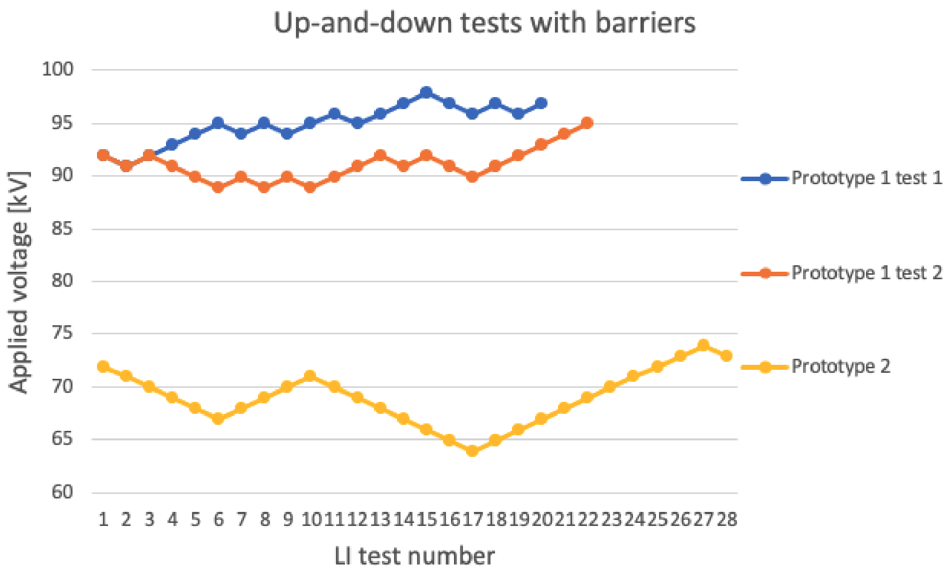

Figure 4.1: Up-and-down results for the tests with barriers.

The reference 50% voltage is within the range of the standard deviations for all tests. There is no significant increase in the breakdown strength for either of the prototypes. The barriers were not tight enough around the cylinder without barriers breaking, meaning that the breakdown voltage is the same with and without a barrier.

4.1.1 Breakdown path

Studying the breakdown channels can indicate the streamer paths and why the breakdown voltage does not increase with barriers. The breakdown channels were either located at the intersection between the two barrier halves, seen in figure 4.2a, or on the inside of the barrier neck, as in figure 4.2b. When the breakdown channels are between the two barrier halves for prototype 1 there is also some indication that there are streamers along the wings of the barrier.

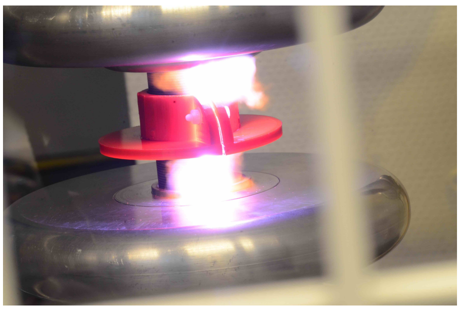

(a) Barrier prototype 1 during breakdown. The barrier is positioned 1.8cm up from the toroid. 95kV applied voltage.

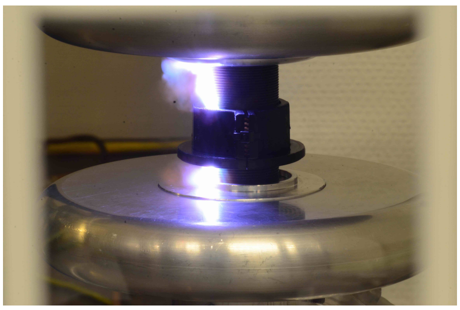

(b) Barrier prototype 2 during breakdown. The barrier is positioned 1cm up from the toroid. 68kV applied voltage. Strips are used.

Figure 4.2: Images of breakdown with barriers.

The increase in breakdown strength from increasing the streamer path is not accomplished with these barriers. The profiled pattern on the barrier neck and the cylinder is not enough to stop the streamers from propagating between them. The tighter the barrier was fastened, the higher the probability was for the nylon screws to break. Regardless of how tight the barrier was fastened, the barrier could not be tightened enough to stop the streamers from propagating on the inside of the barrier neck.

The influence of the dielectric cylinder could be the reason that the breakdown channels are not lead around the barriers. Positive streamers have previously been shown to be attracted to the insulating cylinder by polarisation, electron emission and the surface charge accumulated on the cylinder. The streamers propagate along the cylinder rather than the surrounding air without a barrier, reducing the chance of the streamer propagating around the barrier when there is a barrier.

The two barriers were placed at different heights from the sharp edge. The placement of the barrier has little influence on the breakdown strength when the streamers travel on the inside of the barrier neck. The barrier placement can influence the length of the shortest streamer path but does not happen when the streamer path follows the dielectric cylinder in these experiments. The placement of the barrier could influence the electric field, by changing the geometry of the air gap, and will be studied further in section 4.1.2.

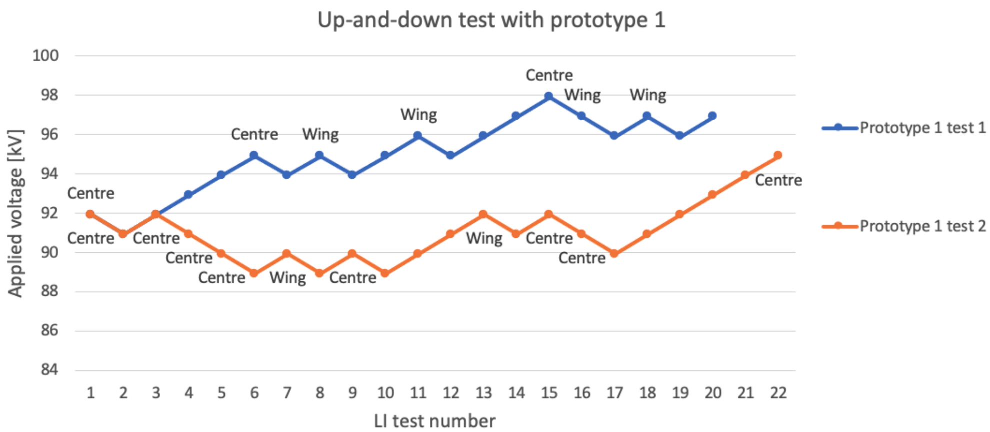

Figure 4.3: Up-and-down results for prototype 1 with the placement of the breakdown channels. 'Wing' indicates that the breakdown channel is placed at the wing between the two barrier halves as seen in figure 3.5. Breakdown at the wings can be seen in figure 4.2a. 'Centre' means the breakdown channel is located at one barrier half, between the wings, where the sharp edge is closest to the cylinder. Breakdown in the centre can be seen in figure 4.2b.

Studying where the breakdown channels are located for the tests for prototype 1, as seen in figure 4.3, can help understand why there is an increase in the breakdown voltage during the up-and-down tests. The increase in breakdown strength is present for the entire first test, while not present until later in the second test. More of the breakdown channels are located at the wings of the barrier when the breakdown voltage is higher, which happens more for the first test. Streamers are generally initiated at the part of the sharp edge with the lowest inception voltage, at the centre of the barrier. When streamers are initiated at the centre of the barriers, they could be arrested by the barrier or the square-profiled cylinder. The electric field could also be weakened due to the accumulation of surface charges on the barrier from previous discharges, increasing the inception voltage at the centre of the barrier. The inception voltage is higher where the wings are located since the distance from the sharp edge to the cylinder is bigger at the wings. When the breakdown channel moves through the wings, the inception voltage is likely higher because the distribution of the electric field has changed. This will gradually increase the breakdown voltage throughout an up-and-down test if the surface charges are not removed.

4.1.2 Simulations of barriers

Table 4.2: Simulated inception voltages at the sharp edge with a square-profiled cylinder with $\epsilon_r = 4.1$. Distance between the sharp edge and the edge of the base electrode is $0.5mm$. Placements can be seen in figure 4.4 .

Placement of barrier [cm]	Inception voltage [kV]	Increase compared to reference [%]
No barrier	66.44	-
1	63.89	-3.8
2	64.01	-3.7

Simulations of the second prototype can be used to understand why the barriers do not behave as expected. The inception voltage in table 4.2 is lowest with the barrier 1cm from the base toroid and increases when the barrier is placed 2cm away from the base electrode. The highest inception voltage occurs when there is no barrier in the gap, which shows that the barrier can increase the field enhancements at the triple junction. In theory, the breakdown voltage should then decrease when a barrier is placed in the gap. This decrease is not found in the experimental results as seen in table 4.1. Streamer propagation could be the dimensioning streamer mechanism for these barriers, explaining why the reduced inception voltage with barriers is not shown in experimental results. When there is a barrier, the streamers are arrested by the barrier and only a few of the streamers actually propagate between the barrier and the cylinder. The fact that fewer streamers can bridge the gap, can increase the voltage required for the streamers to create breakdown, slightly increasing the breakdown voltage with a barrier.

As seen in figure 4.4, showing the electric field with and without the barrier, the electric field is around 0.9V/m at the inner sharp edge for all instances. The differences in the electric field between the barrier placements are not very significant. The electric field is slightly higher in the area between the sharp edge and the barrier, from the shape of the barrier distorting the electric field, which could explain the decrease in inception voltage with a barrier.

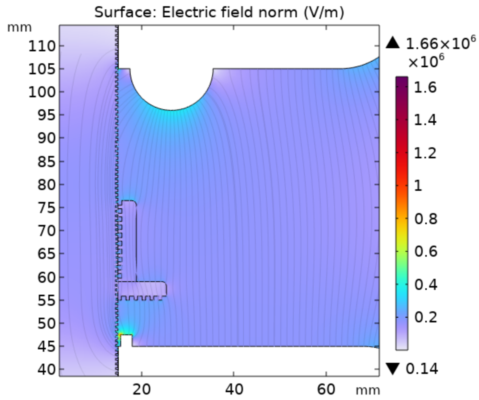

(a) *Electrical field of the barrier placed* 1cm *from the base toroid.*

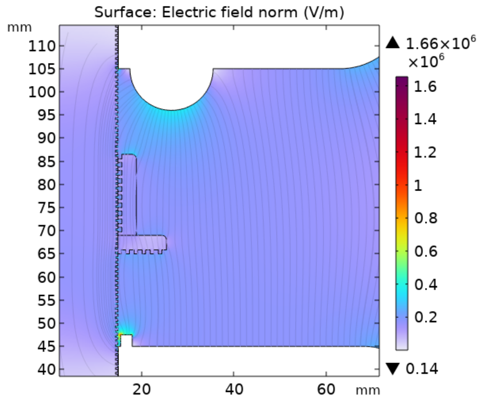

(b) *Electrical field of the barrier placed* 2cm *from the base toroid.*

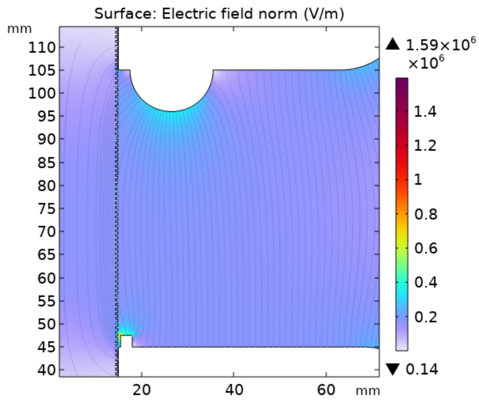

(c) *Electrical field without barrier.*

Figure 4.4: The electric field of prototype 2 in V/m. Simulated with the sharp edge 0.5*mm from the edge of the base electrode,* 0.6*mm from the insulating cylinder. The insulating cylinder has* $\epsilon_r = 4.1$ *and a square surface profile. The PLA barrier is simulated with* $\epsilon_r = 2.675$.

Although these barriers did not increase the breakdown strength significantly, barriers have increased the breakdown strength in previous research. A different design of the barrier is possible to create but should eliminate the discharges moving on the inside of the barrier. A solution could be using a gasket on the inside of a barrier or making a barrier of a more malleable material to fit better around the cylinder, as well as finding a way to eliminate the use of nylon screws or use stronger nylon screws. One solution is to create the cylinder and barriers out of a single material, completely eliminating the possibility of streamers propagating on the inside of the barrier.

4.2 Rubber gaskets

This section aims to answer the second research question about whether rubber gaskets can be used to improve the breakdown voltage of an air gap with a triple junction.

Four different rubber gaskets presented in section 3.1.2 were added to the insulating cylinder at a pure triple junction. The gaskets were placed in milled slots as seen in figure 4.5. The insulating cylinder used in this section is the smooth profiled, POM-cylinder without fibreglass. The cylinder has two milled slots for the gaskets to fit into.

(a) O-ring 3 in the top milled slot. Some gaps are shown between the gasket and slot.

(b) The square gasket in the top milled slot.

Figure 4.5: The electric field of all the rubber gaskets.

4.2.1 Breakdown voltage of rubber gaskets

When studying the rubber gaskets at the triple junction, a breakdown voltage reference is needed for the POM-cylinder without fibreglass and without surface profiles, with a pure triple junction as the electrode. Three reference tests were completed where the milled slots were placed approximately 1cm down from the triple junction without the rubber gaskets. There was grease on the insulating cylinder around the milled slot. The results can be seen in figure 4.6. The three tests develop differently but stabilise around the same area for the last LIs. Reference test 2 is the most stable and is within the range of the two others. Test 2 is chosen as the reference test for the rubber gaskets.

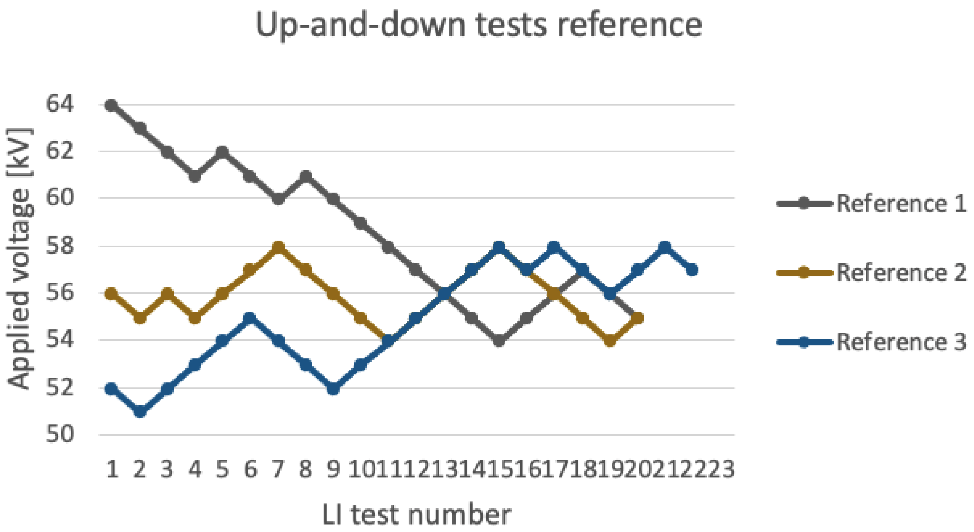

Figure 4.6: Up-and-down results for the reference tests.

The variations in the reference tests reduce the reliability of the tests with gaskets, indicating that minor differences could affect the breakdown voltage. Several factors can explain the differences between the reference tests. For instance, the tests were completed at different times, and the test object was taken apart and reassembled between tests to change the gaskets. The act of reassembling the test object could lead to slight differences in heights between the electrodes or the centring of the cylinder. The insulating cylinder could be placed more to one side for one of the tests, creating different distances between the cylinder and the triple junctions, leading to spots around the cylinder with a higher inception voltage. It could also be explained by the grease added to the insulating cylinder, as some greases can be electrically conductive and would lead to a lower breakdown strength. The grease affects the tests with the gaskets more than without since the grease is further away from the triple junction for the reference tests. It is difficult to conclude, for sure, what causes this difference without further testing of for example the surface charges.

Multiple tests were completed for each gasket. The results can be seen in table 4.3. The first tests for each O-ring show a slight decrease in breakdown strength and there were variations in the results with the same gasket. One of the reasons for these variations could be the grease that was gradually removed when changing the gaskets. The grease was attempted removed but was likely not adequately removed for the first tests of each of the O-rings and could be the reason for the increase in breakdown strength throughout the tests. The most reliable tests are, therefore, the later tests.

Only considering the second test for all gaskets, table 4.3 shows that the third O-ring has the largest increase in breakdown voltage. The square gasket has the lowest increase. The standard deviations are quite large, making the first O-ring the only rubber gasket to have an increase in breakdown voltage where the reference test is not within the range of the estimated standard deviation.

Table 4.3: The 50% breakdown voltage and standard deviations of the test object with the rubber gaskets. With the flat electrode geometry.

Gasket type and test	U_{50} [kV]	σ_{est} [kV]	Increase compared to reference [%]
Reference	55.92	1.84	-
O-ring 1 test 1	55.42	3.69	-0.89
O-ring 1 test 2	58.47	2.25	4.47
O-ring 2 test 1	54.91	3.19	-1.81
O-ring 3 test 1	54.34	1.68	-2.83
O-ring 3 test 2	61.84	10.35	10.59
O-ring 3 test 3	61.41	6.12	9.82
Square test 1	56.06	6.32	0.25
Square test 2	57.50	6.14	2.83

The small increase in breakdown voltage for the second test of O-ring 1 can indicate that O-ring 1 does increase the breakdown voltage to some extent. Taking the standard deviations into account, the increase is more uncertain. Considering the first test and the variations between the reference tests, small variations on the test object could affect this increase in breakdown voltage.

O-ring 2 does not affect the breakdown voltage enough to be of significance. The second O-ring was only tested with grease, meaning there is a chance that an increase in breakdown strength could occur if a test without grease was completed. The second O-ring was also the only O-ring where a second O-ring in the lower slot was not added. The cylinder was likely less centred for this test, contributing to the decrease in inception voltage.

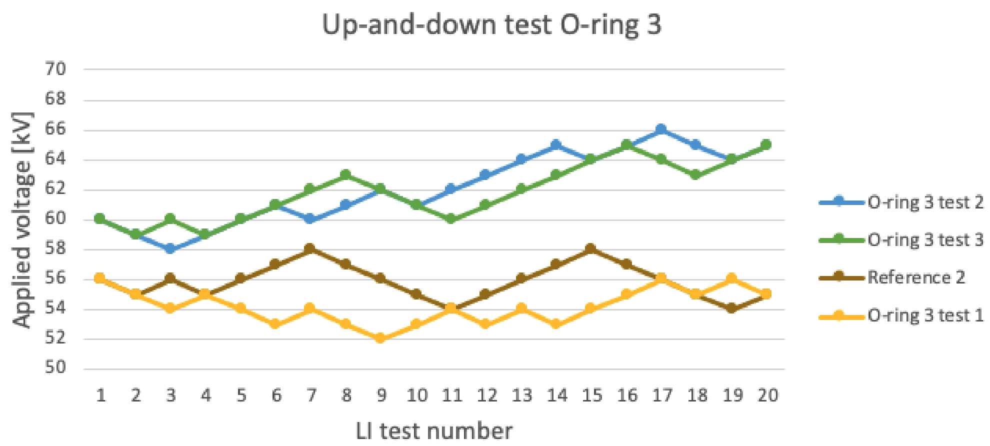

Figure 4.7: Up-and-down results for O-ring 3.

The two last tests for O-ring 3 show a large increase in the breakdown voltage. The estimated standard deviation is large for these tests, and the up-and-down test can be seen in figure 4.7. The two last tests have a high increase in voltage throughout the tests. Interestingly the pattern is very similar for the two tests, starting at the same voltage. This means there is some influence of the previous LI on the next LI, perhaps surface charges. Even with the large standard deviations, the last two tests seem to have some increase in breakdown strength when looking at the up-and-down tests.

The square gasket did not increase the breakdown voltage significantly. The square gasket should be the least affected by the placement of the gasket since the square shape will not alter the electric field as much as a rounded edge. The square gaskets used in the experiments had an uneven edge creating local field enhancements. Studying where the breakdown channels are located for the square gaskets, it can be observed that there is a strong tendency for the inception to occur on one side of the test object and at a few of the same points, confirming that these imperfections cause field enhancements. There is likely also some reduction in the breakdown strength from the grease used to force the gasket into the triple junction.

The dielectric properties of the cylinder and gasket could be the reason for the varying results, especially the tests with large standard deviations were likely strongly affected by the surface charges of the previous LIs. Perhaps the insulating cylinder without fibreglass is more affected by surface charges or polarisation than the cylinder reinforced with fibreglass. The cylinder without fibreglass had traces of the streamers after the tests, while the other cylinder did not, indicating that this cylinder was more affected by the breakdowns.

4.2.2 Breakdown channels

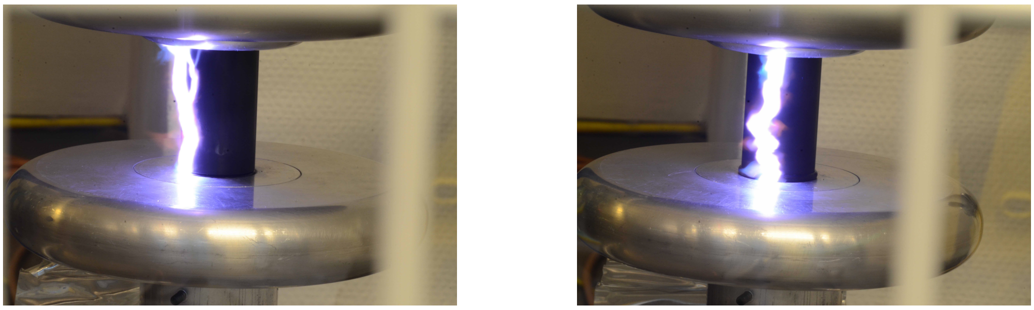

(a) Breakdown channel whit O-ring 1. 55kV charging voltage.

(b) Breakdown channel whit O-ring 2. 60kV charging voltage.

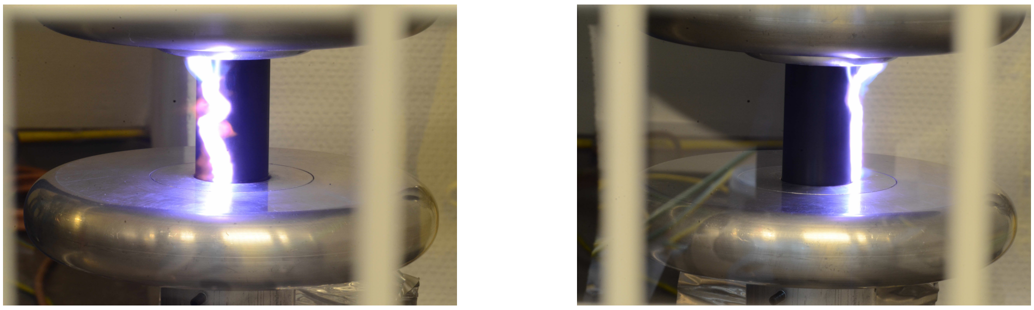

(c) Breakdown channel with O-ring 3. 65kV charging voltage.

(d) Breakdown channel with square gasket. 58kV charging voltage.

Figure 4.8: Images of the breakdown channels for the tests with O-rings.

Studying the breakdown channels seen in figure 4.8 can also give an understanding of the different gaskets. The streamer inception happens around the triple junction for all rubber gaskets. The streamers are positive and propagate toward the negatively charged electrode along the insulating cylinder. The breakdown channels are initiated in no more than three different places for each test. Since the breakdown channels are placed at only a few spots, there is likely unevenness in the gaskets or the placement of the gasket. For instance, the gaskets could be centred differently for each test, creating areas where the cylinder and triple junction are at the critical distance, where the field enhancements are strongest. The second O-rings used to centre the cylinder were not effective since there is no difference between the number of places of initiation for the gaskets that use and do not use a second gasket.

There is a possibility that the breakdown channels shift the placement of the gaskets since it has been observed that there is enough energy during breakdown to break screws as seen in section 4.1. Which could contribute to the larger standard deviations of some of these tests. This is likely not the case when the breakdown channels are located at only a few spots for each test, indicating that the inception voltage is low at only a few points that remain the same for the entire test.

4.2.3 Inception voltage of rubber gaskets

The inception voltages for some of these gaskets were found and presented in this section to compare with the results of the up-and-down tests.

The trends of the inception voltages are more important than the actual voltages in this section, since the inception voltages in table 4.4 and figure 4.10 are mostly higher than the actual breakdown voltages. This contradicts the streamer inception theory when inception occurs at the triple junction. One reason could be that there is another critical point where inception starts. Another reason could be that the insulating cylinder without fibreglass has a lower breakdown voltage than the cylinder with fibreglass. The difference in permittivity between the cylinders is not large enough to be the source of this difference. The reason for this is out of the scope of this paper and needs further testing, but perhaps there are more surface charges on this cylinder affecting breakdown. Using a different insulating cylinder could perhaps lead to a stronger improvement on the breakdown strength with rubber gaskets since there is an increase in inception voltage when using the gaskets compared to without.

Table 4.4: Simulated inception voltages at the triple junction with a smooth rod with $\epsilon_r = 4.1$. Placed where they are attempted placed in the up-and-down tests. Gaskets simulated with $\epsilon_r = 10.8$.

Type of gasket	Inception voltage [kV]	Increase compared to reference [%]
No gasket	62.46	-
O-ring 1	65.21	4.4
O-ring 2	108.61	73.9
O-ring 3	86.39	38.3
Square	120.60	93.1

From the simulation results in table 4.4 and figure 4.9 the square gasket has the highest inception voltage, opposite of what was found in the experiments. A simulation where the square gasket is moved 0.5mm down reduces the inception voltage to 101.23kV. This reduction appears because the field enhancements are increased when the gasket is placed below the intersection. The placement in the actual experiments is likely closer to this distance. The inception voltage is also large compared to the breakdown voltage. The small imperfections in the square gasket can lead to a lower breakdown voltage of the actual gasket. The added grease could also be part of the reason for the lower breakdown voltage.

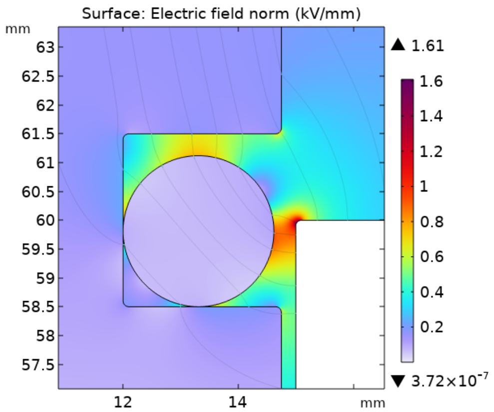

(a) Electric field of O-ring 1. The electric field is around 1.2kV/mm at the triple junction.

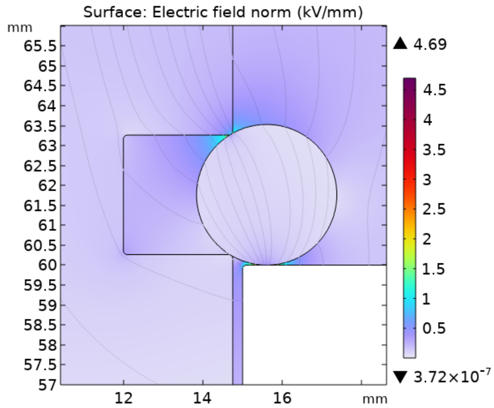

(b) Electric field of O-ring 2. The electric field is around 1kV/mm at the triple junction.

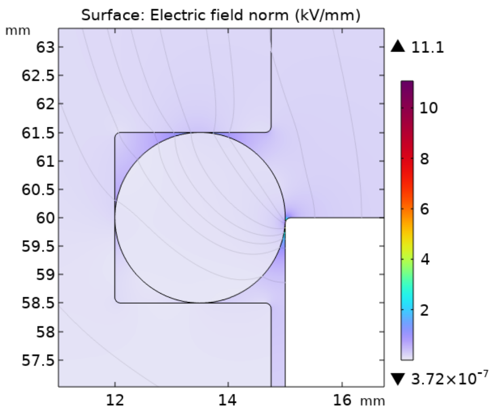

(c) Electric field of the O-ring 3. The electric field is around 1kV/mm at the triple junction.

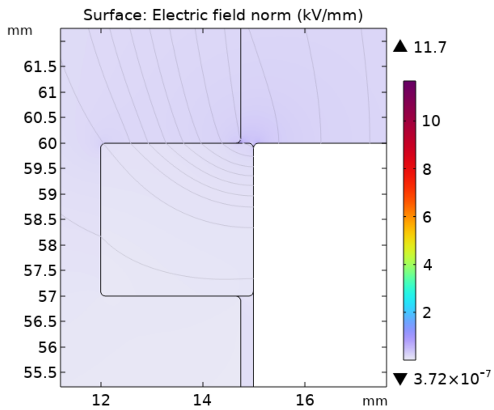

(d) Electric field of the square gasket. The electric field is around 0.8kV/mm at the triple junction.

Figure 4.9: The electric field of all the rubber gaskets.

The O-ring size is important as the third O-ring gives a higher inception voltage than the first O-ring, which is too small for the milled slot. This is likely because the gap between the gasket and the triple junction increases and increases the field enhancements as seen in figure 4.9a. There are also field enhancements between the cylinder and the O-ring. This confirms the suspicion from the up-and-down tests, that the gasket that fits the slot the best, has the biggest increase in breakdown voltage. O-ring 1 is the only O-ring to have around the same increase in inception voltage and U_{50}, meaning that the simulations closely resembled the real situation for this O-ring. The O-rings were stretched when placed in the slots. The simulations of the third gasket are ideal simulations. The third O-ring could also have been too small for the slot and created field enhancements that reduce the influence of adding gaskets, similar to O-ring 1.

The second O-ring has the largest increase in inception voltage compared to the breakdown voltage of the up-and-down tests. The O-ring covered the triple junction in the simulations. The inception voltage is smaller at the toroid, at 106.11kV. It is still larger than the voltage in the up-and-down tests and the breakdown channels seem to start around the triple junction. The dimensions in the simulations are likely, not exact and the gasket is probably stretched and moved to fit better for the real situation, which could explain some of the difference. The difference is, however, very large and must be explained by other factors as well. For instance, the insulating cylinders have low breakdown voltage compared to the cylinder with fibreglass and grease on the insulating cylinder.

As seen in figure 4.10, there are large variations in the inception voltage based on the placements of O-ring 3. Placing the gasket slightly below the intersection like in figure 4.11c will give a higher inception voltage than slightly above the intersection. The electric field differs based on the placement of the gasket as seen in figure 4.11. Placing the gasket slightly above the triple junction like in figure 4.11b means that there are field enhancements below the gasket, creating a volume where dielectric materials surround the triple junction, explaining how this placement is worse than not having a gasket. These differences in placement could be the reason for the results of the up-and-down tests not giving a clear answer as to whether rubber gaskets work, as the placement was not easy to control.

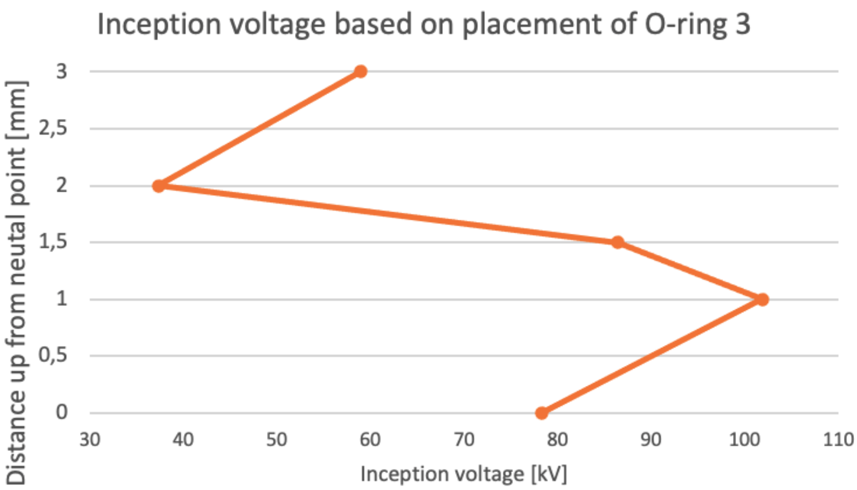

Figure 4.10: Simulated inception voltages with O-ring 3 and smooth cylinder with $\epsilon_r = 4.1$.

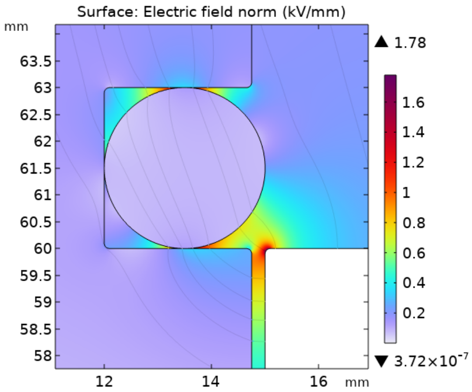

(a) Electric field of O-ring 3, placed 3mm up from the neutral point. The electric field is around 1.4kV/mm at the triple junction.

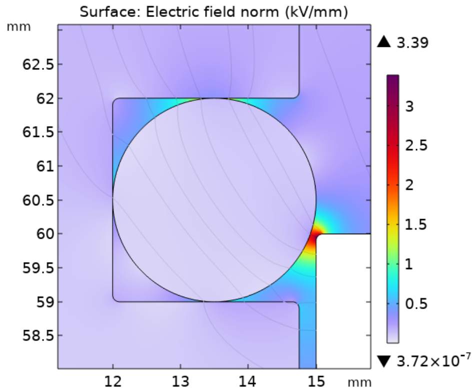

(b) Electric field of O-ring 3, placed 2mm up from the neutral point. The electric field is around 3kV/mm at the triple junction.

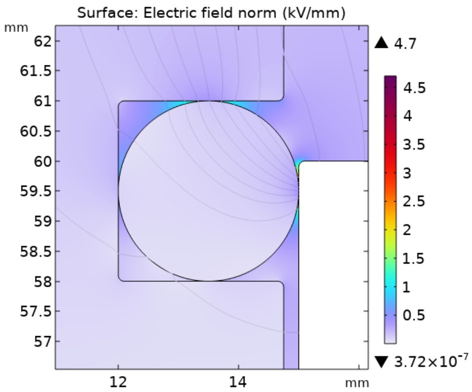

(c) Electric field of O-ring 3, placed 1mm up from the neutral point. The electric field is around 1kV/mm at the triple junction.

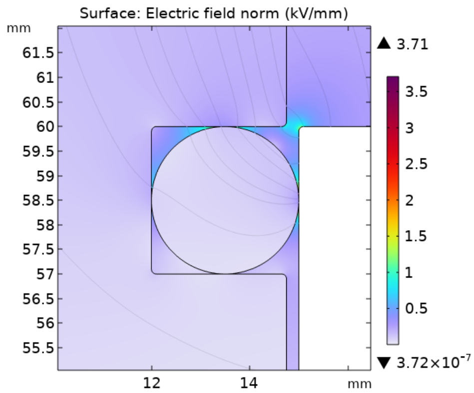

(d) Electric field of O-ring 3, placed at the neutral point (at 0mm). The electric field is around 1kV/mm at the triple junction.

Figure 4.11: The electric field of O-ring 3 at different placements at the triple junction.

4.3 Silicone gaskets

This section aims to answer the two last research questions on whether using silicone gaskets at the triple junction can help increase the breakdown strength of the solid-gas interface under LIs and AC voltage.

Silicone gaskets are made by casting silicone directly on the test object between the cylinder and the symmetrical sharp edge. The insulating cylinder used is the smooth-profiled POM-cylinder with fibreglass.

4.3.1 LI breakdown voltage of silicone gaskets

Table 4.5: The 50% LI breakdown voltage and standard deviations of the test object with the silicone gaskets.

Gasket type	U_{50} [kV]	σ_{est} [kV]	Increase compared to reference [%]
Reference	96.66	2.38	-
Silicone 1	119.30	0.18	23.42
Silicone 2	118.27	0.88	22.36

The results of the up-and-down LI tests for the silicone gaskets are seen in table 4.5. The results indicate a strong improvement in the breakdown voltage. The difference in breakdown voltage between the two silicone gaskets is insignificant, but there is a strong improvement compared to the reference. There are some variations in the test setup from changing the silicone gaskets, like the distance between electrodes and the placement of the electrodes in the gaskets that can explain some of the differences. Two different electrodes and cylinders are used. They are made to the same measurements and should be the same, but could be a source of error.

Small air bubbles in the first silicone gasket from the casting and the uneven edge of the second silicone gasket did not negatively affect the breakdown voltage. These imperfections could have led to field enhancement, but the low permittivity of the gaskets likely reduced this effect.

Comparing the increase in breakdown voltage for the silicone gaskets to the increase in breakdown voltage for the rubber gaskets in table 4.3, the silicone gaskets have a larger increase. Since the silicone gaskets cover the entire triple junction, as opposed to only parts of the triple junction as the rubber gaskets do. The silicone gaskets are also less affected by the placement of the gasket and imperfections in the gasket.

4.3.2 Breakdown channels

The placements of the breakdown channels can give an explanation as to why the silicone gaskets increase the breakdown strength of the gap. Although the silicone gaskets have about the same breakdown voltage, the breakdown channels are located in different areas of the air gap. Most of the breakdown channels for the uncut gasket are further out from the cylinder than the cut silicone gasket, as seen in figure 4.12. A possibility is that the streamers are initiated at the upper electrode and propagate as negative streamers to the base toroid for the uncut gasket. The negative streamer then propagates away from the dielectric. It is likely because the inception occurs further from the insulating cylinder, making the streamer less attracted to the cylinder.

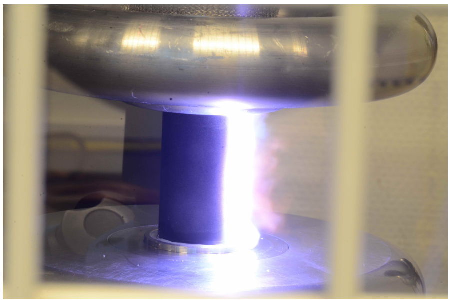

(a) Breakdown channel when silicone gasket 1 is used. 119kV charging voltage.

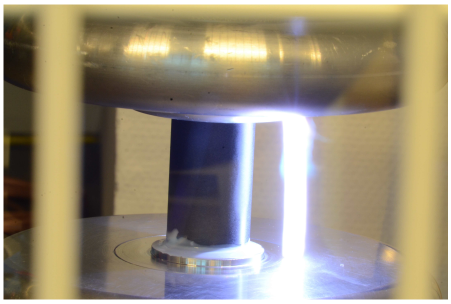

(b) Breakdown channel when silicone gasket 2 is used. 118kV charging voltage.

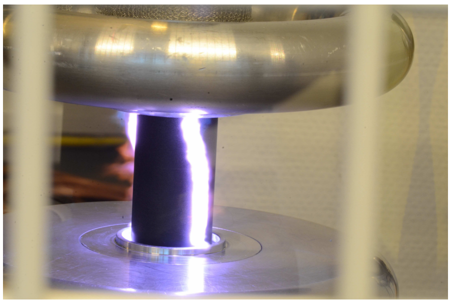

(c) Breakdown channel without silicone gasket. 99kV charging voltage.

Figure 4.12: Images of the breakdown channels for the tests with silicone gaskets compared to without.

Without the silicone gasket, inception seems to occur at the triple junction or on the inside of the sharp edge as seen in figure 4.12c. This is likely where the electric field is highest and the silicone seems to eliminate inception occurring here.

4.3.3 Simulations of silicone gaskets

Simulations of the silicone gaskets are completed to compare with and explain the phenomena that occur with silicone gaskets.

The results of the simulations of the silicone gaskets are presented in table 4.6. As expected, the lowest inception voltage is at the triple junction without a gasket. The lowest inception voltage for the first silicone gasket is expected at the inner sharp edge but is located at the base toroid. For the second silicone gasket, where the inception voltage is lowest at the base toroid, the inception voltages coincide with the experimental results seen in figure 4.12b.

Table 4.6: Inception voltage for the silicone gaskets. Simulations, where inception would lead to the gasket puncturing, are excluded. $\epsilon_r = 3.8$.

	Inception voltage [kV]			
	Triple junction	Inner sharp edge	Outer sharp edge	Base toroid
No gasket	83.83	88.25	109.80	110.23
Silicone 1	-	110.29	114.88	109.06
Silicone 2	-	-	125.71	110.30

The images of the electric fields around the sharp edge in figure 4.13 show a reduction in the electric field when a silicone gasket is placed between the sharp edge and the insulating cylinder. Indicating that inception will occur at a higher voltage with gaskets, corresponding to the increase in the inception and breakdown voltage. The gaskets create a reduction in the field enhancements around the triple junction.

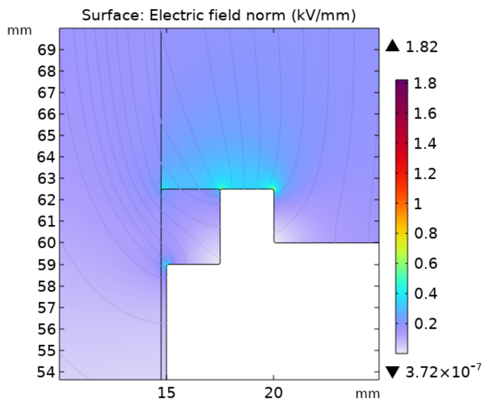

(a) Electric field of the first silicone gasket. The electric field is around 0.5kV/mm at the sharp edge.

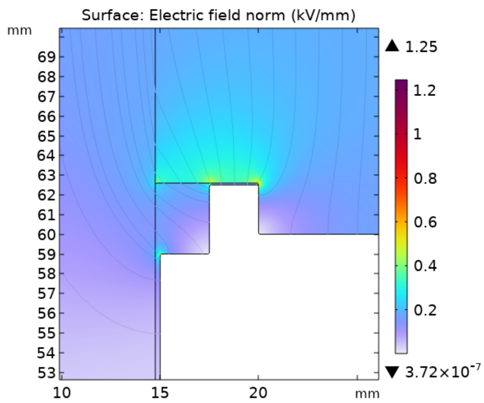

(b) Electric field of the second silicone gasket. The electric field is around 0.4kV/mm at the sharp edge.

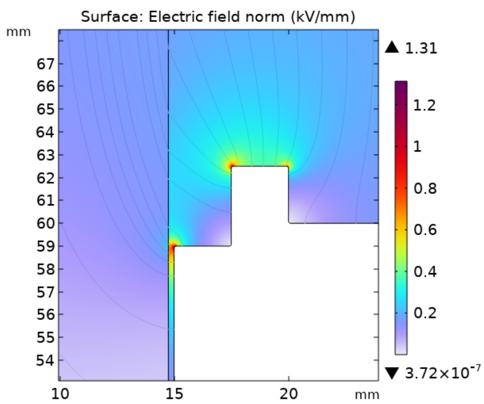

(c) Electric field of the symmetrical sharp edge without the gasket. The electric field is around 1kV/mm at the sharp edge.

Figure 4.13: The electric field of all the silicone gaskets and the symmetrical sharp edge without the silicone gasket.

Table 4.7 shows the inception voltages when inception starts at the upper electrode. With the polarity of the LIs as in the experiments in table 4.5, if inception stating at this electrode leads to a breakdown, the streamers would be negative. As seen in the table, the silicone gaskets both have their lowest inception voltage at the upper triple junction, and the upper rounded electrode is roughly the same as the lower electrode.

Table 4.7: Inception voltage for the silicone gaskets when inception starts at the upper electrodes. $\epsilon_r = 3.8$. The upper electrode is the half circle.

	Inception voltage [kV]	
	Upper Triple junction	Upper rounded electrode
No gasket	96.40	109.31
Silicone 1	94.51	111.75
Silicone 2	93.35	112.70

Comparing the inception voltages to the withstand voltages of the air gap, the streamer propagation is likely sustained for both positive and negative streamers. The voltage for streamer propagation is found using equation (2), for positive streamers $U_w \approx 49.89$, when $U_0 = 23.7$ and $d = 48.5$mm. This is lower than the inception voltage for all cases. When inception occurs, positive streamer propagation should also be sustained. With $E_{st} = 1.2$kV/mm for negative streamer propagation, $U_w \approx 84.9$kV when $d = 51$mm for negative streamers propagating from the top electrode to the base toroid. The voltage required for negative streamer propagation is closer to the inception voltages but is likely still sustained. The distance between the two triple junctions is slightly longer and increases the withstand voltage to 96.9kV for negative streamers. This could explain why the breakdown channels do not seem to propagate from the upper triple junction for the second silicone gasket even when the inception voltage is lowest at there.

For the first silicone gasket the streamers seem to initiate at the inner sharp edge or upper triple junction like in figure 4.12a for the experimental results. The inception voltage is lowest at the upper triple junction, if inception starts there, the streamers would propagate as negative streamers. The voltage would have to be higher than approximately 96.9kV for this to happen. The difference in inception voltage between the top electrode and the lower electrode is 14.55kV, and there is a possibility that the streamers start at the upper triple junction and the negative streamers are sustained. The LI breakdown voltage in figure 4.5 is larger than both inception voltages, meaning that there is still a possibility that the streamers start at the inner sharp edge. It is not possible to conclude for certain how the streamers propagate without using a high-speed camera to capture the streamers.

For the second silicone gasket with the silicone covering the sharp edge, it is likely that the streamer inception occurs at the top electrode as seen from the electric field in figure 4.14. From images like in figure 4.12b, it is known that breakdown channels are not created by from streamers initiated at the triple junctions, although the top triple junction has the lowest inception voltage. Excluding the upper triple junction, the inception voltage is lowest at the toroid. The electric field at the rounded electrode is larger than at the base toroid. The streamer integral is likely solved from the top electrode in the script where α is the highest. Negative streamers initiated at the top electrode cause a breakdown with the second silicone gasket.

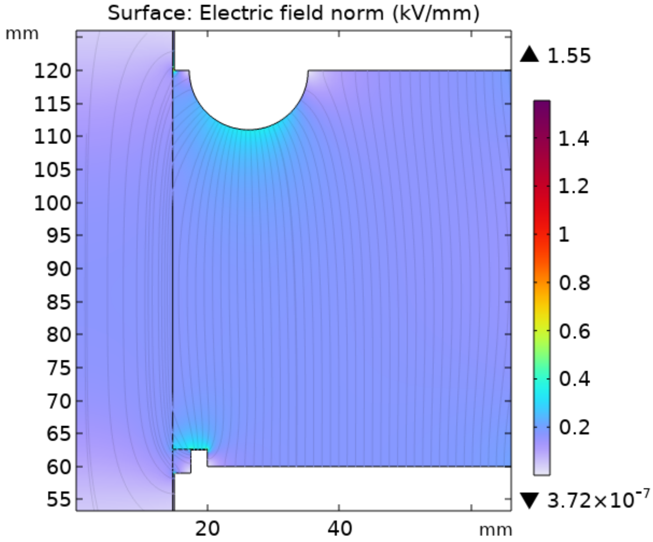

Figure 4.14: The electric field of the second silicone gasket with the other electrode.

The simulation results correspond to the practical situation, where the breakdown voltage is slightly higher than the inception voltage. The U_{50} voltage is around 10kV larger than the inception voltage. U_{50} is not expected to be exactly the same as the inception voltage as it is the lowest possible voltage for where breakdown can occur. Since the standard deviation is low and the electric field is quite homogeneous for the bulk of the air gap, a 10kV increase is a little high when streamer inception is the dimensioning streamer mechanism. There could be slight errors in the simulations compared to the experiments, the permittivity of the components and the electrode distance could explain this difference.

4.3.4 Breakdown voltage of AC stressed silicone gaskets

Any added elements to the GIS must not negatively affect the breakdown strength during normal operation. Therefore, it is important to ensure that the silicone gaskets don't decrease the breakdown strength during AC operation or create any other issues. The average breakdown voltage in table 4.8 shows an increase in the breakdown voltage when the gaskets are added and even an increase between the two gaskets.

Table 4.8: The RMS value of the average AC breakdown voltage for the test object with the silicone gaskets.

Gasket type	$U_{avg,RMS}$ [kV]	Increase compared to reference [%]
Reference	51.80	-
Silicone 1	59.93	15.69
Silicone 2	64.04	23.63

The breakdown strength is improved with gaskets, especially the second silicone gasket. The difference is not as apparent when studying the individual breakdowns in figure 4.15. The trend is an increase in breakdown voltage when there is a gasket and a slight increase with the gasket overlaying the sharp edge, but the lower and higher points of each test are close. The difference is, as for the lightning impulses, explained by differences in the test object as the two gaskets use different cylinders and electrodes or the variations in the electrode distance.

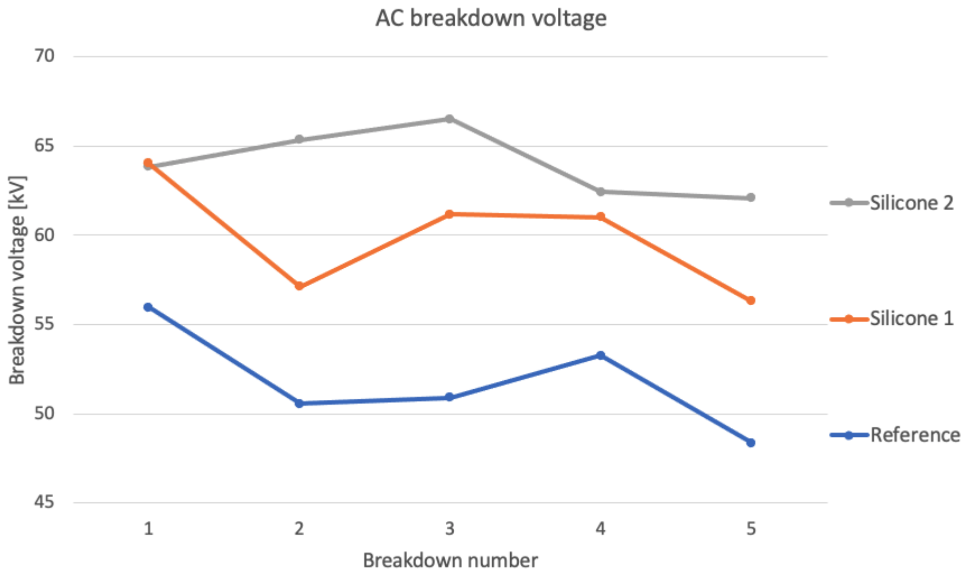

Figure 4.15: The AC breakdown voltage for the silicone gaskets and a reference with five breakdowns each.

Table 4.9: Number of breakdowns for each polarity of the AC breakdown tests. The polarity is considered at the top electrode.

Gasket type	Positive polarity	Negative polarity
Reference	5	0
Silicone 1	4	1
Silicone 2	0	5

Interestingly, the breakdown occurred during the positive half cycle for the reference test and the first silicone gasket, but during the negative half cycle for the second silicone gasket, as seen in table 4.9 when the polarity is considered at the upper electrode. Breakdowns usually occur during the positive half-cycle, where the streamers are initiated on the positive electrode. When positive streamers cause the breakdowns, the streamers are initiated at the top electrode when there is no gasket and at the sharp edge with the second silicone gasket. The first silicone gasket is between the two cases, but mostly the streamers are initiated at the top electrode. The opposite is expected when comparing streamer inception to the lightning impulses and the simulations. The streamers with the second gasket are more likely to start at the top electrode when this electrode is positive. The simplest explanation is that the voltage is measured at the opposite polarity than expected since the voltage was measured using the voltmeter integrated variac. It is difficult to know for certain what polarity this voltmeter is connected to and the oscilloscope was likely connected to the voltmeter at the opposite polarity. This would mean that the polarity is considered at the sharp edge, not the top electrode as is shown in table 4.9.

The negative polarity for silicone gasket 2 is caused by positive streamers initiated at the top electrode, not the sharp edge. Without a gasket, positive streamers are initiated at the sharp edge. For the first silicone gasket, streamers can initiate at both the top electrode and the sharp edge, but they are mostly initiated at the sharp edge.

4.3.5 Ageing of the gaskets

After the AC voltage tests, small black spots on the silicone gaskets appeared, visible in figure 4.16. Most of them went away after scraping, and no signs of punctures were visible. In an actual situation under normal operations, unknown particles could be an issue in GIS. Particles in an enclosed insulation system would remain and could interfere with components in the switchgear. Using other materials could be tested to see if it is an issue with the material or whether it is related to the breakdown itself.

Figure 4.16: Image of the second silicone gasket after AC testing, where small black particles are visible on the gasket.

There were more particles on the second silicone gasket than on the first silicone gasket. It is a possibility that the particles appear when the streamers travel from the top electrode to the silicone gasket at the sharp edge during a negative polarity breakdown. The black spots can consist of particles from the negative streamer reaching the silicone gasket. The spots could also be from the heat generated by the breakdowns since the silicone looks scorched at some spots close to the sharp edge. The loose particles will then have been created at this spot and scattered along the gasket.

5 Conclusion

To conclude, the research questions presented in section 1.1 are answered below:

1. 3D-printed PLA barriers, made as two parts with a barrier and a neck connected with nylon screws, around an insulating cylinder will not increase the breakdown strength of the gas-solid interface. This is because the breakdown channel is located between an insulating cylinder and a barrier.

2. Rubber gaskets can improve the breakdown voltage of the air gap with an insulating cylinder, but minimal variations in the placements and type of gaskets could decrease this effect. The gasket would have to be big enough and placed precisely where the inception voltage would increase most, around 1mm up from the neutral point. The cylinder should also be centred. Simulations of rubber gaskets indicate that the correct placement of the gasket could increase the inception voltage by 38% when using an O-ring that fits the gap perfectly at the correct placement. Achieving this increase in real situations is not possible.

3. Silicone gaskets have a 20% increase in breakdown voltage compared to a reference setup for an air gap with a solid-gas interface. The increase in inception voltage around the triple junction is the main reason for this increase, eliminating the field enhancement at the triple junction. Two silicone gaskets are tested, one cut and one uncut. The streamers are initiated at the top electrode for the uncut silicone gasket and propagate as negative streamers. For the cut silicone gasket streamers are initiated at the inner sharp edge of the bottom electrode and propagate along the dielectric surface as positive streamers or from the upper triple junction and propagate as negative streamers to the sharp edge. The inception voltage for these gaskets is roughly the same, and propagation is maintained for both the negative and positive streamers. The increase in breakdown voltage is the same for both silicone gaskets.

4. Testing the same gaskets in an AC-stressed situation, they have a slightly higher breakdown voltage and do not negatively affect the breakdown strength during regular operation. However, small particles that appear during AC testing could cause issues when using silicone gaskets.

6 Further Work

Based on the work completed in this thesis, some further research may include:

- The 50% breakdown voltage and streamer mechanisms could be studied in other air compositions or under pressure to understand discharge behaviours in different air compositions.
- Performing the same experiments captured with a precise high-speed camera to further study the pre-breakdown mechanisms with the development of streamers and leaders.
- A study of how and why different material compositions of the insulating cylinder affect the breakdown voltage of the air gap could be completed. Using a high-speed camera, it is possible to see if the streamer development is different with different material compositions or if it changes the streamer attraction.
- Investigating a barrier that is an integrated part of the cylinder.
- Testing whether adding silicone or a malleable material between the barriers and cylinders can stop the breakdown channels from moving through the barrier neck.
- Further study of the gaskets effect on triple junctions, perhaps studying surface charges on the triple junctions.
- Studying the combination of surface profiles and the silicone gasket to test whether the two effects could be combined, especially with the cut silicone gaskets where streamers propagate along the insulating cylinder.
- Completing an up-and-down test with negative polarity at the sharp edge for the silicone gaskets could be interesting to see if positive streamers initiated at the top electrode appear and how the breakdown strength is affected by the polarity change.
- Investigating the ageing of silicone gaskets at the triple junction. Implementing, for instance, a photomultiplier tube (PMT) to trigger a regular camera or high-speed camera to capture the breakdown channels or streamers during AC operation could help understand why particles appear on the silicone gasket. The PMT could also be used to detect partial discharges before breakdown. Using an IR camera to see if there is excess heating of the silicone could help understand if there is ageing of the gasket.

Bibliography

[1] ECHA, European Chemicals Agency. 'Echa publishes pfas restriction proposal'. (), [Online]. Available: https://echa.europa.eu/-/echa-publishes-pfas-restriction-proposal (visited on 5th Jun. 2023).

[2] H. G. Osberg, 'New environmentally-friendly insulation gases – breakdown mechanisms along insulating rods', *Specialisation Project Report, Department of Electric Energy, Norwegian University of Science and Technology (NTNU)*, 2022.

[3] E. Ildstad, *TET4160 Insulating Materials for High Voltage Applications.* NTNU Department of Electric Power Engineering High Voltage Technology Research Group, 2022.

[4] S. Nijdam, J. Teunissen and U. Ebert, 'The physics of streamer discharge phenomena', *Plasma Sources Science and Technology*, vol. 29, 2020. DOI: https://doi.org/10.1088/1361-6595/abaa05.

[5] A. Pedersen, T. Christen, A. Blaszczyk and H. Boehme, 'Streamer inception and propagation models for designing air insulated power devices', in *2009 IEEE Conference on Electrical Insulation and Dielectric Phenomena*, 2009, pp. 604–607. DOI: 10.1109/CEIDP.2009.5377740.

[6] H. K. H. Meyer, *Dielectric barriers under lightning impulse stress. Breakdown and discharge-dielectric interaction in short non-uniform air gaps.* PhD thesis. Norwegian University of Science and Technology, 2019.

[7] R. Van Brunt, E. Cernyar and P. von Glahn, 'Importance of unraveling memory propagation effects in interpreting data on partial discharge statistics', *IEEE Transactions on Electrical Insulation*, vol. 28, no. 6, pp. 905–916, 1993. DOI: 10.1109/14.249364.

[8] H. K. H. Meyer, R. Marskar, H. Bilsbak, F. Mauseth and M. Schueller, 'Streamer propagation along profiled insulator surfaces under positive impulse voltages', *Proceedings of the Nordic Insulation Symposium*, vol. 27, 2022. DOI: https://doi.org/10.5324/nordis.v27i1.4494.

[9] H. K. Meyer, R. Marskar, H. Osberg and F. Mauseth, 'Surface flashover over a micro-profiled cylinder in air', *IEEE Transactions on Dielectrics and Electrical Insulation*, pp. 1–1, 2023. DOI: 10.1109/TDEI.2023.3277413.

[10] S. M. Lebedev, O. S. Gefle and Y. P. Pokholkov, 'The barrier effect in dielectrics: The role of interfaces in the breakdown of inhomogeneous dielectrics', *IEEE Transactions on Dielectrics and Electrical Insulation*, vol. 12, no. 3, 2005. DOI: 10.1109/TDEI.2005.1453459.

[11] X. Meng, H. Mei, L. Wang, Z. Guan and J. Zhou, 'Characteristics of streamer propagation along insulation surface: Influence of shed configuration', *IEEE Transactions on Dielectrics and Electrical Insulation*, vol. 23, no. 4, pp. 2145–2155, 2016. DOI: 10.1109/TDEI.2016.7556489.

[12] A. Goldman, M. Goldman, E. Odic and P. Dessante, 'Partial discharges inception and ageing effects in a gas insulated hv equipment', in *2008 17th International Conference on Gas Discharges and Their Applications*, 2008, pp. 49–56.

[13] *Powersil® xlr® 630 a/b*, Wacker, 2022.

[14] North Star High Voltage. 'High voltage probes'. (), [Online]. Available: https://www.highvoltageprobes.com/products/high-voltage-probes/ (visited on 2nd Nov. 2022).

[15] *Technical data - impulse voltage test system ipf 5/200 lr*, 526765 DS, HighVolt, 2018.

[16] IEC, 'IEC 60060-1:2010 High- voltage test techniques - Part 1: General definitions and test requirements', 2010.

[17] *Record of performance according to iec 60060-2*, 526765 20367678, HighVolt, 2018.

[18] W. Hauschild and W. Mosch, *Statistical Techniques for High-Voltage Engineering*. The Institution of Engineering and Technology, 1992, IET Power series 13, ISBN: 9780863412059.

[19] *P5200a series high voltage differential probes, instruction manual*, Tektronix, 2004.

[20] D. Yang, X. Kong, Y. Ni *et al.*, 'Novel nitrile-butadiene rubber composites with enhanced thermal conductivity and high dielectric constant', *Composites Part A: Applied Science and Manufacturing*, vol. 124, p. 105 447, 2019, ISSN: 1359-835X. DOI: https://doi.org/10.1016/j.compositesa.2019.05.015. [Online]. Available: https://www.sciencedirect.com/science/article/pii/S1359835X19301903.

[21] K. Petcharaks, *Applicability of the streamer breakdown criterion to inhomogenous gas gaps*. PhD thesis. ETH Zürich, 1995. DOI: https://doi.org/10.3929/ethz-a-001507778.

Appendix

A Results from previous research

Some relevant results from the preliminary project are presented below.

A.1 The influence of surface profiles on breakdown voltage

Table A.1: U_{50} and standard deviation in kV from up-and-down test. The increase in breakdown voltage about the smooth profile was calculated. Voltage is corrected for atmospheric conditions for the applied voltage. Positive polarity air gap.

Profile	U_{50} **[kV]**	σ **[kV]**	**Increase in** U_{50} [%]
Smooth	66.14	1.01	-
Semi-circular	70.76	4.97	7.0
Rectangular	91.13	10.75	37.8

B Inception voltage

B.1 Inception voltage equations

For air, the Petcharacks values for $\alpha(|E|)$ are found using the equations below [21].

When $7.943 > E/p > 14$kV/mm bar $\alpha(|E|)$ is found using equation (9):

$$\frac{\alpha}{p} = C_1\left(\frac{E}{p}\right) - A_1, \tag{9}$$

where $C_1 = 16.77661/\text{kV}$ and $A_1 = 80.00061/\text{mmbar}$.

When $2.588 < E/p < 7.943$kV/mm bar it is found using equation (10):

$$\frac{\alpha}{p} = C\left[\frac{E}{p} - \left(\frac{E}{p}\right)_M\right]^2 - A, \tag{10}$$

where $C = 1.6053\text{mm bar/kV}^2$,$(E/p)_M = 2.165\text{kV/mm bar}$, $A = 0.2873$ l/mm bar, and $(E/p)CT = 2.588$ kV/mm bar.

When $E/p < 2.588$kV/mm, $\alpha = 0$.

B.2 Python script

```
#!/usr/bin/env python3
# -*- coding: utf-8 -*-


"""
Created on Fri Jan  5 17:00:44 2018

@author: hans.meyer@sintef.no

Written by Hans Kristian Meyer and Julia Glaus.
This script calculates streamer inception voltages along field lines in air,
air+ or sf6, using fit functions mainly from Petcharaks PhD thesis, 1995.

Field lines are generated from COMSOL simulations.
The input is either a field line with electric field strength in kV/mm and distance
in x and y directions in mm from a 2D or 3D simulation. Also,
the applied voltage and pressure must be given. 10 kV and 1 bar is default.
```

```

Place the CSV field lines you want to calculate in the chosen folder and run
python inception.py.

For help run python inception.py --help

The default output file is inception.txt.

Currently only the standard COMSOL export formats is accepted.

Also, the script estimates breakdown voltage based on propagation distance
U = E_st*d + U_0, where E_st = 0.54 kV / mm, U_0 = 23.7 kV


"""

import pytest  # for testing
import numpy as np
from abc import ABC, abstractmethod
import glob
import os
import pandas as pd
import argparse
parser = argparse.ArgumentParser()
parser.add_argument('-m', '--medium', type=str, default='air',
                    help="air, air+, or sf6. Default air")
parser.add_argument('-p', '--pressure', type=float, default=1,
                    help="in bar. Default 1")
parser.add_argument('-v', '--voltage', type=int, default=10,
                    help="applied voltage in kV. Default 10")
parser.add_argument('-f', '--file', type=str, default='inception.txt',
                    help="filename for outfile. Default inception.txt ")
parser.add_argument('-fo', '--folder', type=str, default='./',
                    help="folder with fieldlines. Default ./ ")
args = parser.parse_args()


class Line(ABC):
    """
    Generic abstract class for electric field lines.
    The output format of the calculated field lines may differ, so this class
    is only meant as a template for a field line.
    """
```

```python

    @abstractmethod
    def get_values(self, line):
        return

    def __init__(self, file, delim, voltage):
        return

    def get_inception(self, line):
        """
        This function calculates inception voltage.
        Integrates the ionization coefficient for the given gas and pressure.
        If the resulting integration does not exceed the given streamer
        constant, the field is scaled up.
        """
        if self.medium == 'air':
            STREAMER_CONSTANT = 9.15  # for ionization integral (log(N) where
            # N is the critical number of electrons required to initiate a
            # streamer in air)
        elif self.medium == 'air+':
            STREAMER_CONSTANT = 12.9
        elif self.medium == 'sf6':
            STREAMER_CONSTANT = 10.15

        U = self.voltage  # applied voltage in kV
        P = self.pressure  # pressure in bar
        k = 0.01  # voltage scaling factor
        STEP_SIZE = 0.001  # Increase voltage scaling factor if inception is
        # not achieved
        C = 0  # counter
        u_i = 0  # Inception voltage
        iteration_counter = 0
        while C < STREAMER_CONSTANT:
            #  Scale field
            field = self.E*k

            # Start at high field end of field line
            if field[-1] > field[0]:
                field = np.flip(field)
            #  FIND ALPHA
            alpha = np.zeros(len(field))
            for i in range(len(field)):
                if self.medium == 'air':
```

```
                        # (from Julia Glaus?)
                        # if field[i]/P > 14:
                            # alpha[i] = (1175 * np.exp(-28.38 * field[i] / P)) * P
                        # # From Petcharaks
                        # if field[i]/P > 7.943 and field[i] / P <= 14:
                        if field[i]/P > 7.943:
                            alpha[i] = (16.7766 * (field[i] / P) - 80.006) * P
                        if field[i]/P >= 2.588 and field[i] / P <= 7.943:
                            alpha[i] = (1.6053*(field[i] / P - 2.165) ** 2 - 0.2873) * P
                        if field[i]/P < 2.588:
                            break

                    elif self.medium == 'air+':
                        # From ABB?
                        if field[i] / P > 10:  # Valid to 19.2
                            alpha[i] = (19.452 * field[i] / P - 118.48)*P
                        if field[i] / P >= 5.53 and field[i] / P <= 10:
                            alpha[i] = (17.418 * field[i] / P - 97.46) * P
                        if field[i]/P < 5.53:
                            break

                    elif self.medium == 'sf6':
                        # From Petcharaks
                        if field[i] / P >= 12.36:  # kV/mm Valid to 21 kV/mm
                            alpha[i] = (22.359 * field[i] / P - 180.171) * P
                        if field[i] / P >= 8.9246 and field[i] / P < 12.36:
                            alpha[i] = (27.9 * (field[i] / P - 8.9246)) * P
                        if field[i]/P < 8.9246:
                            break

                    else:
                        print('Please choose a medium. air, air+ or sf6')

                # INTEGRATE ALPHA
                C = np.trapz(alpha, self.dist)

                # SCALE UP VOLTAGE
                u_i = U*k

                # INCREMENT SCALING FACTOR
```

```
            k = k+STEP_SIZE
            iteration_counter += 1

        return u_i

    def get_propagation(self):
        """
        This function calculates breakdown voltage in air based on the streamer
        propagation (stability) criterion.
        """
        return 0.54*self.length + 23.7


class FieldLine(Line):
    """
    This class takes  field line in the format (x coordinate, y coordinate,
    (optional) z coordinate, field line number, field strength, dimension),
    which is the standard output format of COMSOL Multiphysics.
    This class inherits the Line() class
    """

    def __init__(self, line, applied_voltage, pressure, medium, dim):
        self.dimension = dim  # dimension
        self.voltage = applied_voltage
        self.pressure = pressure
        self.medium = medium
        self.get_values(line)
        self.u_i = self.get_inception(line)
        self.Uprop = self.get_propagation()

        return

    def get_values(self, line):
        # line = np.stack(line)
        self.x = np.asarray(line['x'])
        self.y = np.asarray(line['y'])
        self.E = np.asarray(line['E'])
        if self.dimension == 3:
            self.z = np.asarray(line['z'])
        self.get_distance()

    def get_distance(self):
        self.dist = np.zeros(len(self.x))
        dl = np.zeros(len(self.x))
        if self.dimension == 2:
```

```
            for i in range(0, len(self.x)-1):
                dl[i] = np.sqrt((self.x[i+1] - self.x[i])**2 +
                                (self.y[i+1] - self.y[i])**2)
                self.dist[i+1] = self.dist[i]+dl[i]
            self.length = self.dist[len(self.dist)-1]
        elif self.dimension == 3:
            for i in range(0, len(self.x)-1):
                dl[i] = np.sqrt((self.x[i+1] - self.x[i])**2 +
                                (self.y[i+1] - self.y[i])**2 +
                                (self.z[i+1] - self.z[i])**2)
                self.dist[i+1] = self.dist[i]+dl[i]
            self.length = self.dist[len(self.dist)-1]


class ComsolReader:
    """
    This class reads .csv files from COMSOL. If the file contains several field
    lines, the reader will split them up. Check out template files in this
    repo.
    """

    def __init__(self, file, delim):
        self.f_lines = []
        df_meta = pd.read_csv(file, sep=r',', nrows=7, index_col=0,
                              header=None).T  # metadata
        self.dim = int(df_meta['% Dimension'].values[0])
        print(self.dim)
        self.comsol_model = df_meta['% Model'].values[0]
        print('{2}\n The file {0} comes from COMSOL simulation {1} \n{2}\n\n\n'
              ''.format(file, self.comsol_model, '='*50))
        self.comsol_type = df_meta['% Description'].values[0]
        df = pd.read_csv(file, skiprows=7)  # read data to pandas dataframe

        if self.dim == 2:  # 2D file
            df = df.rename(columns={'% x': 'x', '% r': 'x', 'z': 'y',
                                    'Color': 'E', 'Electric field norm': 'E'})
            # name columns according to COMSOL Multiphysics export format

        if self.dim == 3:   # 3D file
            df = df.rename(columns={'% x': 'x', 'Color': 'E'})

        if self.comsol_type == 'Streamline':
```

```python
            for j in range(max(df['Streamline']) + 1):
                self.f_lines.append(df[df['Streamline'] == j])  # split the
                # bundle in new dataframe for each fieldline
        if self.comsol_type == 'Line':
            self.f_lines.append(df)


class InceptionCalculation():
    """
    This class performs calculation of inception voltages on a list of field
    lines
    """

    def __init__(self, in_files_list, out_file, applied_voltage, pressure,
                 medium):
        self.in_files_list = in_files_list
        self.df = pd.DataFrame()
        print(in_files_list)
        if os.path.isfile(out_file):
            os.remove(out_file)
        else:
            pass
        self.out_file = out_file
        self.voltage = applied_voltage
        self.pressure = pressure
        self.medium = medium
        self.get_inception()
        self.write_to_file()

    def get_inception(self):
        for file in self.in_files_list:
            self.calculate_file(file)

    def calculate_file(self, file):
        incs = []  # list of inception values for each field line
        bundle = ComsolReader(file, ',')  # Read the bundled file from COMSOL
        [field_lines, dim, comsol_model] = [bundle.f_lines,
                                            bundle.dim,
                                            bundle.comsol_model]
        count = 1
        for line in field_lines:
            if dim == 2:  # 2D file
                inc = FieldLine(line, self.voltage, self.pressure,
                                self.medium, dim).u_i
```

```
                print('For {}D field line {} the inception voltage in {:.2f} '
                      'bar {} is: {:.2f} kV'.format(dim, count, self.pressure,
                                                    self.medium, inc),
                      end="\r")
                incs.append(inc)
                count += 1
            if dim == 3:  # 3D file
                inc = FieldLine(line, self.voltage, self.pressure, self.medium,
                                dim).u_i
                print('For {}D field line {} the inception voltage in {:.2f}'
                      'bar {} is: {:.2f} kV'.format(dim, count, self.pressure,
                                                    self.medium, inc),
                      end="\r")
                incs.append(inc)
                count += 1

        data = {'Filename': file,
                'Origin': comsol_model,
                'Dimension': dim,
                'Pressure [bar]': self.pressure,
                'Applied voltage [kV]': self.voltage,
                'Medium': self.medium,
                'No. of lines': len(field_lines),
                # 'Inc. voltages': incs,
                'Min. inception voltage [kV]': min(incs)}

        self.df = self.df.append(data, ignore_index=True)
        self.df = self.df[data.keys()]
        print(self.df)

    def write_to_file(self):
        self.df.to_csv(self.out_file, mode='a', index=False)


if __name__ == '__main__':
    # Find all files *.csv in folder (except the example files for the testing)
    list_of_files = glob.glob('{}/[!example]*.csv'.format(args.folder))
    print(list_of_files)
    out_file = args.file
```

```
    applied_voltage = args.voltage  # kV in COMSOL
    pressure = args.pressure  # bar
    medium = args.medium  # air, air+ or sf6
    calc = InceptionCalculation(list_of_files, out_file,
    ↪  applied_voltage,
                                pressure, medium)
```

NTNU

Norwegian University of
Science and Technology